Stokes Drift Mapping Using a Single High-Frequency Radar

Abïgaëlle Dussol* and Cédric Chavanne*

*Institut des sciences de la mer de Rimouski, Université du Québec à Rimouski, Canada

Surface gravity waves play a major role in coastal circulation and upper-ocean mixing. Waves induce a net drift in the direction of wave propagation known as the Stokes drift. Stokes drift affects multiple processes in the ocean such as wave-induced sediment transport and Langmuir circulation cells responsible for upper-ocean Langmuir turbulence. Moreover, Stokes drift estimations are required to determine Lagrangian velocities, which affect dispersion of pollutants, including oil and biological organisms such as fish larvae. As direct measurement is challenging, Stokes drift is usually estimated from in-situ measurements of directional wave spectra, which limits the spatial resolution of the Stokes drift field. Using in-situ observations of wave spectra by a bottom-mounted Acoustic Wave and Current Profiler (AWAC) deployed in the lower St. Lawrence estuary, and observations of the wind speed and direction at a nearby meteorological station, we show that observed wave spectra closely follow the parametric form proposed by Toba (1979), and can thus be obtained from the wind speed, direction and fetch. We use a new method to estimate the wind field from the first-order Bragg-resonant peaks observed by a single High-Frequency (HF) radar, which we apply to data from a Wellen Radar (WERA) and a Coastal Ocean Dynamics Applications Radar (CODAR) monitoring the location of the AWAC. Two-dimensional maps of Stokes drift are then estimated from the wind field obtained from each HF radar using Toba wave spectra. Correlation coefficients between the radar-estimated and AWAC-estimated Stokes drifts are 0.87 for the WERA and 0.86 for the CODAR.
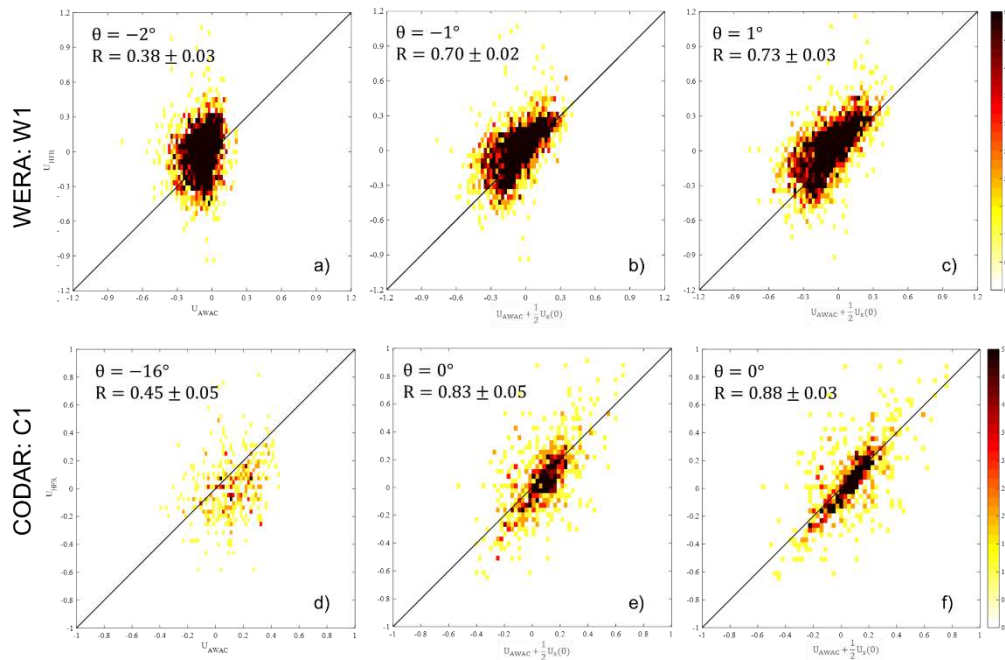

Figure1: Scatterplots of the HF radar radial currents for the WERA W1 (a,b,c) and the CODAR C1 (d,e,f) vs the Eulerian radial currents for the Bic AWAC. In b) and e) half of the surface Stokes drift estimated by HF radar are added to the AWAC currents, and in c) and f) half of the surface Stokes drift estimated by AWAC are added to the AWAC. The correlation coefficients R and the $x = y$ line are indicated in each panel. The colors indicate the number of observations in velocity bins. $\Delta\theta = \theta_{AWAC} - \theta^*$, where θ_{AWAC} is the radar azimuth toward the AWAC and $\theta^*$is the radar azimuth yielding the best comparison with AWAC currents.

Latest Methods for Automated Evaluation & Change Detection of HFR Antenna Response

Dale Trockel, CODAR Ocean Sensors Ltd.
Joshua Trockel, CODAR Ocean Sensors Ltd.
Chad Whelan, CODAR Ocean Sensors Ltd.
Laura Pederson, CODAR Ocean Sensors Ltd.

Extended Abstract—High Frequency surface wave Radars (HFR) are used throughout coastal regions to monitor ocean conditions in near-real time, providing beyond-the-horizon measurements with ranges of up to 300 km. Maintaining high quality HFR surface current measurements is vital for end user applications such as search and rescue, spill response, and ship detection. The quality of HFR surface current measurements is dependent on the accurate measurement of the receiver's antenna response patterns to assign direction of arrival (DoA) to incoming signals. If electromagnetic (EM) conditions at the site morph or hardware changes are made, the antenna response can also be impacted. If not properly factored into the data processing scheme, this leads to the deterioration of the DoA assignment accuracy, regardless of the nature of the receive antenna configuration. At present, there are several methods of measuring the antenna response patterns in the field, the most robust of which involves transporting by foot, drone, or boat a signal source in a path around the antennas to properly characterize the response of the receive antennas to the DoA. Routine manual remeasurement of antenna response patterns for ongoing system QA is generally infrequent, and it is often the case that the measured response patterns remain valid for more than a year without needing to be changed. However, when a change does occur, it is essential to minimize the identification and response time. For a technician with some basic training and a few stations to monitor, this has historically been a straightforward and routine task. As networks grow larger, to dozens of stations in some cases, having automated, quantifiable monitoring and evaluation done for the operator reduces costs and minimizes response time to changes. We present two classes of metrics to monitor and detect changes in the antenna response pattern autonomously.

The monitoring methods fall into two main categories: 1) monitoring and quantifying changes in the distribution of radial surface current vectors (radials) and 2) monitoring the error statistics in DoA assignments.

Hourly and even daily fluctuations in the radial distribution produced by an HFR are normal due to environmental variations, but on average, these fluctuations follow similar trends over longer periods of time. As distributions are averaged and compared over longer periods of time, differences in the distributions become marginal. These changes can be quantified using metrics such as Earth Movers Distance and Kullback–Leibler divergence. Significant changes in these averaged distributions are indicative of EM environment or hardware changes, which may be mitigated by the remeasurement of the antenna response pattern.

In addition to sea echo, HFR Doppler spectra contain echoes from moving vessels in its field of view. These vessel echoes can be matched with information transmitted by the vessels' automatic identification system (AIS) to provide a ground truth for DoA. By comparing the assigned DoA to the ground truth direction, we can quantify the error in DoA assignments, as well as monitor bias in these assignments. When the ground truth direction significantly differs from the assigned DoA, this indicates that the antenna response pattern should be remeasured.

By proactively monitoring the stability and accuracy of an antenna response pattern, the reliability of DoA assignments increases, which can have positive downstream effects on current measurement and other applications of HFR data. Two classes of monitoring metrics for quantifying the reliability of HFR antenna response patterns are discussed, and examples of these monitoring methods that have successfully detected changes and signaled the need to update the antenna response patterns are presented.

High Frequency Surface Wave Radar Studies of Inertial Oscillations in a Coastal Embayment

Joe Craig and Eric Gill
Department of Electrical and Computer Engineering
Brad deYoung
Department of Physics and Physical Oceanography
Memorial University of Newfoundland
St. John's, Newfoundland and Labrador, Canada

Keywords: High frequency radar, currents, model

Extended Abstract – Validation of surface current velocities derived from high frequency surface wave radar (HFSWR) against conventional measurements is challenging because the measurement regimes are largely disparate. Further, the standard deviation of a typical current velocity time series and the mean value are close. Inertial oscillations, recently identified in monostatic HFSWR and current meter records, have motivated us to explore novel means of augmenting validation and further studies.
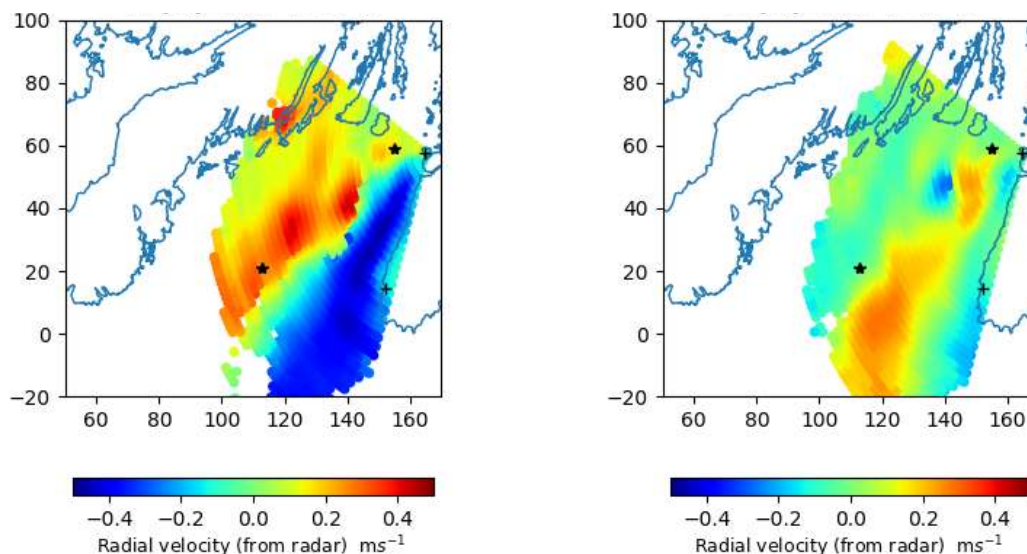
Fig. 1. Placentia Bay (47°N 54°W) coastline and radial HFSWR currents at 1058 and 1813 ut 13 July 2018. The crosses and stars show the positions of the HFSWR and current meters, respectively. The axes labels are in units of km north and east from an arbitrary reference point.

The Radar Remote Sensing Laboratory (RRSL) at Memorial University operates 2 HFSWR facilities in Placentia Bay, Fig. 1. These are frequency modulated continuous wave (FMCW) instruments with 8 and 12 element phased array receive antennas operating at 13.385 MHz with a bandwidth of 50 kHz, yielding azimuthal and range resolutions of about 10° and 3 km respectively.

The Argentia facility (location indicated by the upper cross) has, over the past 10 years, provided data that supported several research initiatives such as improving methods of surface wave

height and surface current estimation. Recent initiatives have included assessment of calibration and processing methods (Wang and Gill, 2015) and system optimisation, such as transmit and receive antenna performance. During the summer of 2018, the HFSWR derived current values exhibited near inertial periodicity following a wind event. Strong density stratification of the water column and a shallow mixed layer depth were optimal for inertial motion; the current reached 0.5 ms^{-1}. Oscillations persisted for 5 cycles with a mean period of 15.3 hr. The local inertial period is 16.4 hr.

Surface current fields at 1058 and 1843 ut, an interval of one half the measured inertial period (Fig. 1) highlighted diverse spatial and temporal structures within the bay. Acoustic Doppler Current Profile (ADCP) instruments showed clear inertial signals at the Mouth of Placentia Bay (MPB lower star) however these were absent at the Red Island mooring (upper star). Inertial motion presented in HFSWR records within 10 km of the mooring.

Agreement between the HFSWR radial current at the range and azimuth of MPB and the corresponding ADCP values was high during the oscillations; the Pearson correlation coefficient exceeded 0.9 but was otherwise close to 0.0. Dissimilarities between the instruments' data time series were generally constrained to the high frequency band ($T <1$ hr) for both data segments. A spectral analysis of a 30 day radial current record from the MPB ADCP was dominated by the inertial band with a slight contribution from the M_2 tidal component.

A simple one dimensional physical model driven by local wind stress (deYoung and Tang, 1990) accounted for most of the inertial variability in the current meter data and reaffirmed the assignment of the observed oscillations to inertial motion. The model enabled indentification and comparison of differences between the two time series.

Brad deYoung, B. and C. L. Tang, "Storm-Forced Baroclinic Near-Inertial Currents on the Grand Bank," *J. Phys. Oceanogr.* 20, pp. 1725–1741, 1990.

Wei Wang and Eric Gill "High-Resolution Spectral Estimation of HF Radar Data for Current Measurement Applications," *J Atmos Ocean Tech.* 32, pp. 1515-1525, 2015.

Surface Aggregation Patches in Coastal Waters Monitored by HF Radar

M.L.Heron[1], T.H.Tran[3], J.Widera[3], H.Peters[2], R.Gomez[3], T.Helzel[3] and P.Dekker[2]

[1]Marine Geophysics Laboratory and Physical Sciences, James Cook University, Australia.
[2] Xi Advies B.V. , Nieuw-Buinen, The Netherlands.
[3]Helzel Messtechnik GmbH, Kaltenkirchen, Germany.

Keywords: HF radar, Lagrangian Tracking, Pollution, Water Quality

Extended Abstract—Pollution and water quality management are among the challenges for coastal oceans in the UN Decade of Ocean Science for Sustainable Development. In particular flotsam and buoyant pollution provide challenges for monitoring and managing near ports and in Marine Protected Areas. The ubiquitous challenge of the monitoring and removal of plastics in the coastal ocean can be addressed by applying high quality HF maps of surface currents. HF radars have been used successfully in seasonal dynamics up to 200km from the coast for coastal circulation, streams and eddies. Tidal dynamics require sampling on at least an hourly schedule and most data archives of HF radar data are using hourly values on 2D grids with resolution of typically 1-3km. In some data sets the integration time is stretched to more than one hour in order to reduce errors to less than $0.1ms^{-1}$. For detection of tsunamis approaching the coast and storm surge monitoring, observations need to be taken at least every few minutes which challenges the accuracy because the integration times are reduced. Increasingly HF radar data is being used for operational purposes, rather than for archiving and research and the data used in this presentation is from an operational HF radar at the Port of Rotterdam.

The HF radar installation returns surface current maps on a 1 km grid every 15 minutes at sufficient precision to enable the calculation of derivative parameters of DIV and CURL, and to carry out Lagrangian tracking of buoyant surface water parcels in the coastal ocean. These parameters are used to track a patch of low salinity water from the Rhine River through a tidal cycle to show an aggregation area near the coast on the north side of the river mouth. The aggregation of river water shown by the HF radar is compared with a satellite Synthetic Aperture Radar (SAR) image, and also with the distribution of chlorophyll-a in the area.

Figure 1(left panel) shows the surface currents on an ebb tide with the contours of CURL showing the vorticity at the edges of the plume. Figure 1 (right panel) shows the surface currents very close to high tide. During the previous flood tide the surface layer of river water has formed the high convergence patch to the north-east of the river mouth and the river flow at the time of this image is still flowing into that north-east patch. Directly in front of the river mouth the new ebb river plume is forming. This presentation follows the development of these river-water systems.
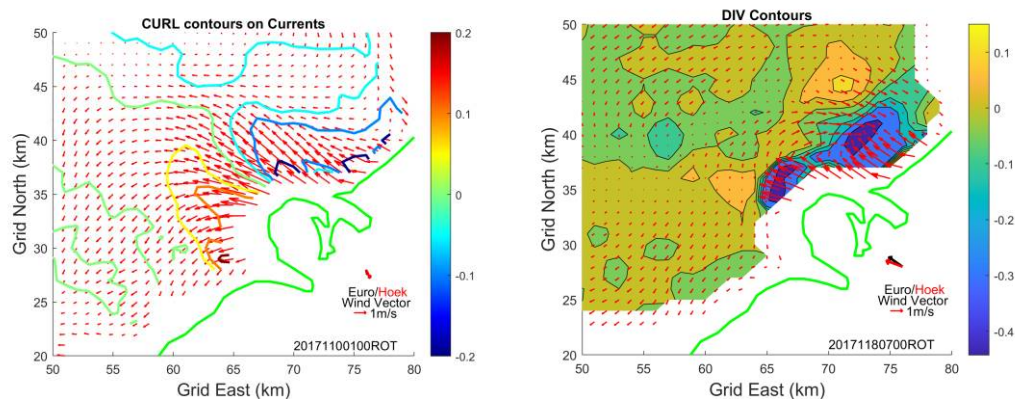

Figure 1. Surface current maps from the WERA HF radar at the Port of Rotterdam produced after a 15 minute integration period. The Left panel shows contours of the CURL operator on the 2D current vector field during ebb tide. The right panel shows contours of the DIV operator near high tide.
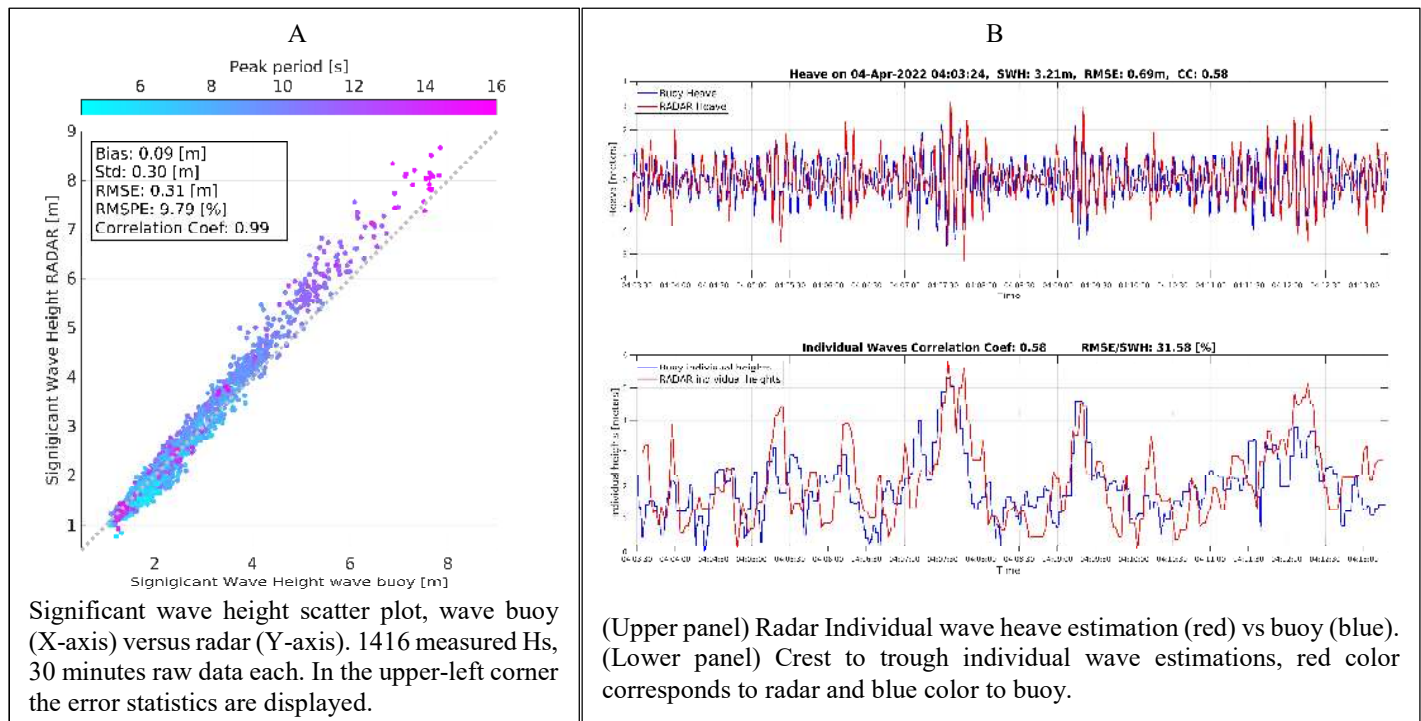
Wave Field Retrieved by Coherent X-band Radar

Ruben Carrasco/ Institute of Coastal Ocean Dynamics, HelmholtzZentrum Hereon
Jose Carlos Nieto-Borge/ Department of Physics and Mathematics, University of Alcala.
Joerg Seemann/ Institute of Coastal Ocean Dynamics, HelmholtzZentrum Hereon.
Jochen Horstmann/ Institute of Coastal Ocean Dynamics, HelmholtzZentrum Hereon.

Keywords: Radar remote sensing, Marine X-band Coherent radar, Individual waves, Sea surface dynamic, Significant wave height retrieval.

Extended Abstract—The determination of significant wave height constitutes a crucial component of the monitoring of the dynamic marine environment, holding significant importance for activities such as oceanic navigation, the maintenance of offshore wind farms, and the preservation of marine resources. The determination of significant wave height from X-band marine radars operating at grazing incidence, typically relies on empirical algorithms that demand calibration, ideally customized for each unique radar configuration. However, this innovative physics-based approach, coherent X-band marine radar data is utilized to retrieved significant wave heights without the requirement for calibration. In contrast to previously published methods, where the antenna had to be pointed into the main wave direction, this approach is utilized with a continuously rotating antenna.

The proposed method is based on the measurement of Doppler speeds from coherent X-band radar, which are associated to the radial horizontal orbital speeds of the surface waves. The resulting orbital speeds are converted via linear wave theory to a wave surface elevation field. Finally, the significant wave height and peak period are computed from the surface elevation field. The method was tested and applied to an extensive data set collected over a period of 29.5 days, covering four storms, at the offshore research platform FINO-3 in the southern North Sea. Comparison of radar retrieved significant wave heights to data obtained by a wave buoy in vicinity of the FINO-3 resulted in a correlation of 0.99, a root mean square error of 0.31 m, and a bias of 0.09 m (Figure A). The same comparison was performed for peak periods, resulting in a correlation coefficient of 0.85, a root mean square error of 1.28 s, a standard deviation of 1.18 s and a bias of 0.5 s. The impact of various sea-state parameters, such as wave breaking, wave steepness, and wind speed, on the estimation of significant wave height is exposed.

In a 3.2 m significant wave height sea state, a wave by wave validation was also performed, comparing the radar retrieved sea surface heave versus the wave buoy radar data (Figure B, upper panel), resulting cross correlation coefficient of 0.58 and a root mean square error of 0.69 m. The individual waves height, crest to trough distance, was also retrieved and is displayed in the Figure lower panel.

Significant wave height scatter plot, wave buoy (X-axis) versus radar (Y-axis). 1416 measured Hs, 30 minutes raw data each. In the upper-left corner the error statistics are displayed.

(Upper panel) Radar Individual wave heave estimation (red) vs buoy (blue). (Lower panel) Crest to trough individual wave estimations, red color corresponds to radar and blue color to buoy.

Enhanced Estimation of Significant Wave Height From Rain-contaminated X-Band Radar Image Sequences

Zhiding Yang, Memorial University of Newfoundland
Weimin Huang, Memorial University of Newfoundland

Extended Abstract—Accurately measuring significant wave height (SWH) in the vast oceans is incredibly important as it directly impacts maritime safety, climate studies, and coastal management. Currently, SWH estimation from X-band radar images has become one of the trending research topics as X-band radar has high spatial and temporal resolution (Dankert et al., 2003), requires low cost and energy consumption, and it can align well with the principles of sustainable development in ocean science. However, as a result of the rain contamination on radar images, the accuracy of significant wave height (SWH) estimation from the radar images collected under rainy conditions is adversely affected (Chen et al., 2022).

This paper presents a novel approach for enhancing SWH estimation from rain-contaminated radar images by combining DehazeNet (Cai et al., 2016) and convolutional gated recurrent unit (CGRU) networks (Chen et al., 2022). The framework of
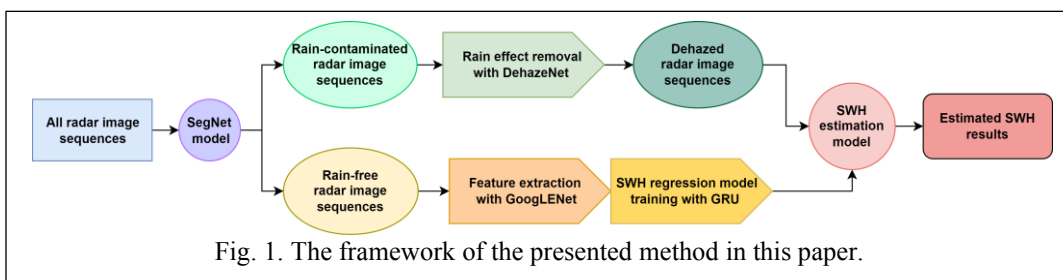

Fig. 1. The framework of the presented method in this paper.

the complete approaches used in this paper is shown in Fig. 1. Firstly, a CNN-based dehazing algorithm, i.e., DehazeNet, is employed to correct the visual degradation caused by rain in the radar images. Subsequently, an advanced deep regression network that combines GoogLENet and GRU architectures is utilized to perform further SWH measurements from the dehazed radar images.

TABLE I: SWH estimation deviation statistics

| | Testing results (Rainy) | | | | | |
| | Without averaging | | | With averaging | | |
	RMSD (m)	CC	Bias (m)	RMSD (m)	CC	Bias (m)
CGRU-based method	0.58	0.91	-0.43	0.53	0.92	-0.40
DehazeNet+CGRU-based method	0.51	0.91	-0.33	0.47	0.93	-0.32

Fig. 2: Scatter plots of the estimated results using the (a) CGRU- and (b) DehazeNet+CGRU-based methods.

The training and testing data used in this study were acquired by a shipborne X-band marine radar in 2008 from a maritime area off the southeastern coast of Halifax, Canada. To validate the effectiveness of the newly introduced dehazing algorithm, the CGRU-based method (Chen et al., 2022) is used for comparison. The root-mean square deviations (RMSDs), correlation coefficients (CCs), and bias results of both methods from the rain-contaminated radar image sequences are presented in Table I. In addition, the scatter plots of the retrieved SWH and the buoy-measured SWH are illustrated in Fig. 2. The RMSD of the proposed method is decreased to 0.47 m, and the CC is increased to 0.93. Thus, the improvement in the results illustrates that the inclusion of a dehazing algorithm can further optimize the performance of SWH estimation from rain-contaminated radar images.
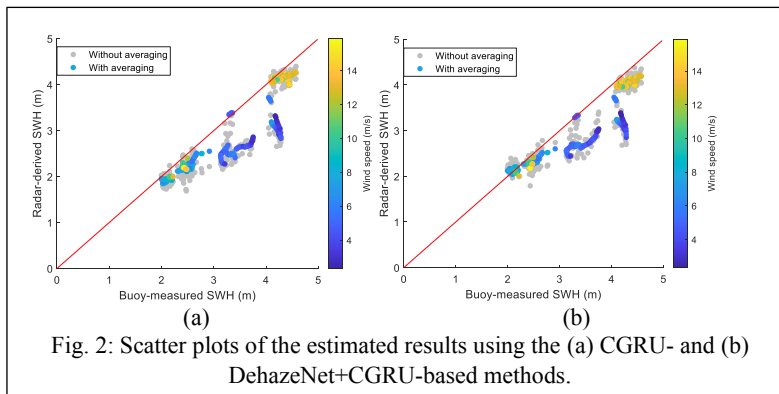
Reference
[1] B. Cai, X. Xu, K. Jia, C. Qing, and D. Tao, "Dehazenet: An end-to-end system for single image haze removal," *IEEE Trans. Image Process.*, vol. 25, no. 11, pp. 5187–5198, 2016.
[2] H. Dankert, J. Horstmann, and W. Rosenthal, "Ocean wind fields retrieved from radar-image sequences," *J. Geophys. Res.*, vol. 108, no. C11, 2003.
[3] X. Chen and W. Huang, "Spatial-temporal convolutional gated recurrent unit network for significant wave height estimation from shipborne marine radar data," *IEEE Trans. Geosci. Remote Sens.*, vol. 60, pp. 1–11, 2022.

Wave Density Spectra Estimation with LSTM from Sentinel-1 SAR in the Baltic Sea

Sander Rikka, Department of Marine Systems, Tallinn University of Technology
Sven Nõmm, Department of Software Science, Tallinn University of Technology
Victor Alari, Department of Marine Systems, Tallinn University of Technology
Martin Simon, Department of Software Science, Tallinn University of Technology
Jan-Victor Björkqvist, Norwegian Meteorological Institute

Keywords: Sentinel-1, Wave Spectra, Baltic Sea, LSTM
Extended Abstract— Many studies have focused on estimating wave spectra from Synthetic Aperture Radar (SAR) imagery. In the open ocean, where high-resolution Wave Mode data capture predominately swell waves, various inverse methods have been developed to extract 2D wave information. However, these methods face limitations in closed wind-wave dominant regional seas like the Baltic Sea, where long-swell waves are lacking, and lower-resolution ScanSAR (TOPS mode for Sentinel-1 (S1)) acquisitions are prevalent.

Recent advancements by Simon et al., 2023 involve the application of recurrent deep learning neural network methods, such as long-short-term memory (LSTM), to estimate 1D wave density spectra from S1 Interferometric Wide Swath (IW) image spectra (*ISP*) data in the Baltic Sea. This study aims to expand the dataset by incorporating NORA3 wave model spectra and training the LSTM network to estimate wave density spectra from S1 IW data within the 2 to 10-second range.

The image spectra are computed from calibrated and speckle-filtered (Frost 5 × 5) S1 IW sub-images (VV and VH polarizations), covering an area of approximately 5 by 5 kilometers. Collected from the beginning of 2015 to the end of 2021, S1 data align with the locations of the model spectra. The WAM-based NORA3 wave model (Breivik et al., 2022) covers the Pan-Arctic domain, including the Baltic Sea, at a 3 km resolution, with spectra output at a 30 km resolution. A total of 165 locations in the Baltic Sea are utilized to extract ISP from SAR data, resulting in an approximately 75,000-data-point training set.

For the LSTM model, a single input has the shape (48, 4), with the four variables being ISP_{VVx}, ISP_{VVy}, ISP_{VHx}, and ISP_{VHy} (x and y correspond to *ISP* range and azimuth direction components). Normalized depth, incidence angle, and satellite pass direction precede each ISP component. The model output is limited to frequencies from 0.1 to 0.46 (36 values with a resolution of 0.01 Hz). Prior to LSTM training, the natural logarithm is applied to ISPs and NORA3 wave spectra. The recurrent neural network model has two hidden LSTM units, the first with 72 and the second with 54 neurons, and the last dense layer with 36 output neurons.
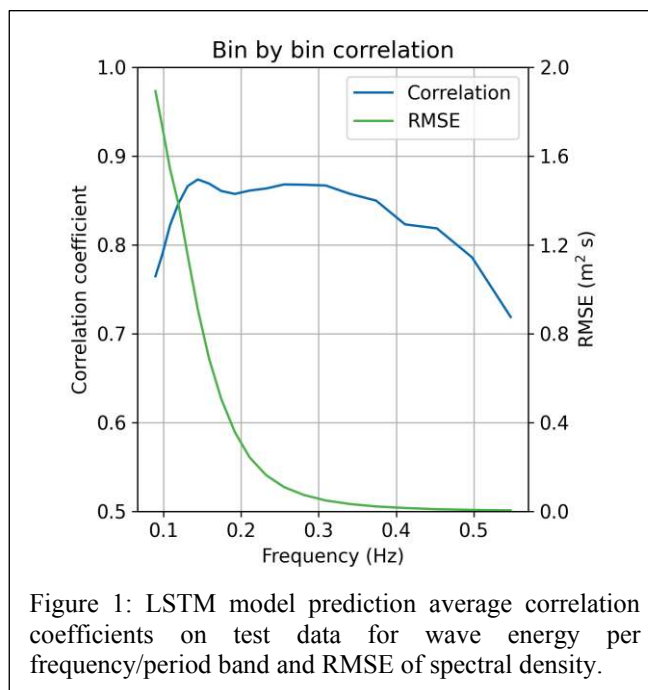

Figure 1: LSTM model prediction average correlation coefficients on test data for wave energy per frequency/period band and RMSE of spectral density.

Results from the LSTM network demonstrate correlations exceeding 0.80 between wave periods of 2 and 9 seconds for the wave density spectra (Figure 1). Root Mean Square Error (RMSE) values of spectral density remain below 0.5 m² s for periods between 2 and 5 seconds. These results show very similar outcomes to Simon et al. (2023), indicating the generalization of the LSTM model for estimating 1D wave spectra from SAR image spectra in the Baltic Sea.

References:

Simon, Martin, Sander Rikka, Sven Nõmm, and Victor Alari. "Application of the LSTM models for baltic sea wave spectra estimation." *IEEE Journal of Selected Topics in Applied Earth Observations and Remote Sensing* 16 (2022): 83-88.

Breivik, Øyvind, Ana Carrasco, Hilde Haakenstad, Ole Johan Aarnes, Arno Behrens, Jean-Raymond Bidlot, Jan-Victor Björkqvist et al. "The Impact of a Reduced High‐Wind Charnock Parameter on Wave Growth With Application to the North Sea, the Norwegian Sea, and the Arctic Ocean." *Journal of Geophysical Research: Oceans* 127, no. 3 (2022): e2021JC018196.

Ocean Swell Height Estimation From Spaceborne GNSS-R Data Using Tree Model Based Machine Learning Methods

Jinwei Bu, Faculty of Land Resources Engineering, Kunming University of Science and Technology, Kunming 650093, China
Qiulan Wang, Faculty of Land Resources Engineering, Kunming University of Science and Technology, Kunming 650093, China
Xinyu Liu, Faculty of Land Resources Engineering, Kunming University of Science and Technology, Kunming 650093, China
Linghui Li, Faculty of Land Resources Engineering, Kunming University of Science and Technology, Kunming 650093, China
Yongfeng Zhang, Faculty of Land Resources Engineering, Kunming University of Science and Technology, Kunming 650093, China
Weimin Huang, Department of Electrical and Computer Engineering, Memorial University of Newfoundland, St. John's, NL A1B 3X5, Canada

Extended Abstract—Swell monitoring is very important in ocean and coastal engineering, ship transportation, coastal protection, and meteorological forecasting. Traditional method of measuring surge height is to use buoys, however, the ability to cover large areas of water is limited. Satellite altimeters are also helpful for measuring swell height, but their temporal and spatial resolutions are low, making real-time swell monitoring challenging (Altiparmaki et al., 2022).

Global Navigation Satellite System-reflectometry (GNSS-R) has opened a new window for swell height measurements due to its short revisit period, low observation cost, and high spatial and temporal resolution (Munoz-Martin et al., 2020). In spite of that, limited research has been dedicated to swell height retrieval. To assess the feasibility of using spaceborne GNSS-R for swell monitoring, Bu et al. (2022) used three observables extracted from CYGNSS DDM data, i.e., DDM average (DDMA), leading edge slope (LES), and trailing edge slope (TES), to estimate swell height for the first time. The results show that the root mean square error (RMSE) and correlation coefficient (CC) between the estimated swell height from the three observables and ERA5 data are 0.56 m and 0.86, respectively. Nevertheless, the model constructed in that study only incorporates a small number of input parameters, resulting in a suboptimal retrieval accuracy. Consequently, this study utilizes spaceborne GNSS-R data from the CYGNSS satellite and machine learning methods based on tree models (i.e. Random Forest (RF), Decision Tree (DT), Gradient Boosting Decision Tree (GBDT), eXtreme Gradient Boosting (XGBoost), and Light Gradient Boosting Machine (LightGBM)) to develop a multivariate regression based swell height estimation model to improve the performance of swell height estimation.
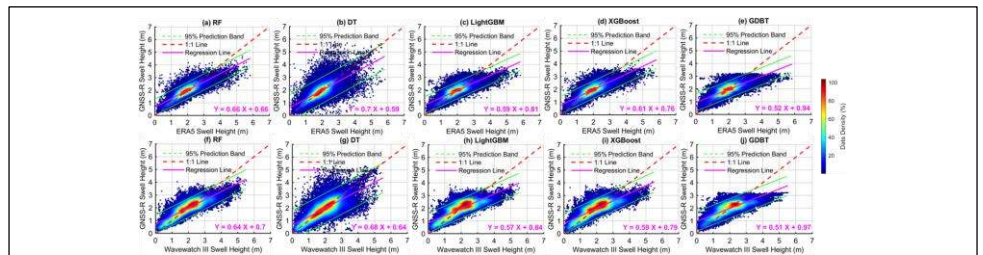

Fig.1 Scatter density plots of different models for inverting swell height and ERA5 and Wavewatch III swell height data.

Tab.1 Performance comparison of different models for inverting swell height and ERA5 and Wavewatch III swell height data

Models	GNSS-R VS. ERA5				GNSS-R VS. Wavewatch III			
	RMSE (m)	Bias (m)	CC	MAPE (%)	RMSE (m)	Bias (m)	CC	MAPE (%)
RF	0.409	-0.004	0.83	16.80	0.491	0.002	0.84	23.00
DT	0.570	-0.001	0.70	21.31	0.658	0.001	0.71	27.30
LightGBM	0.455	0.002	0.78	19.88	0.546	0.008	0.79	27.12
XGBoost	0.451	0.002	0.79	19.24	0.541	0.010	0.79	26.02
GBDT	0.493	0.003	0.74	22.44	0.585	0.003	0.76	30.71

To verify the performance of the proposed models, ERA5 and Wavewatch III (WW3) data are used as reference data for testing. Using RMSE, bias (Bias), CC, and mean absolute percentage error (MAPE) as accuracy metrics. Fig. 1 shows the results of swell height retrieval from different models in comparison with ERA5 and WW3 swell height data ((RMSE, Bias, CC, and MAPE statistical results are listed in Table 1). The results show that when ERA5 is used as reference data, the proposed RF model performs the best in retrieval performance among the five models, with RMSE and CC being better than 0.409 m and 0.83, respectively. When WW3 is used as reference data, the RMSE and CC are better than 0.491 m and 0.83, respectively. The method proposed in this article exhibts great potential for global swell height retrieval using CYGNSS data.

Altiparmaki O, Kleinherenbrink M, Naeije M, Slobbe C, Visser P. (2022). SAR altimetry data as a new source for swell monitoring. Geophysical Research Letters, 49, e2021GL096224.
Bu J, Yu K, Park H, Huang W, Han S, Yan Q, Qian N, Lin Y. (2022). Estimation of Swell Height Using Spaceborne GNSS-R Data from Eight CYGNSS Satellites. Remote Sensing, 14, 4634.
Munoz-Martin JF, Onrubia R, Pascual D, Park H, Camps A, Rüdiger C, Walker J, Monerris A. (2020). Experimental Evidence of Swell Signatures in Airborne L5/E5a GNSS-Reflectometry. Remote Sensing, 12, 1759.

Enhancing the versatility of a 4-beam ADCP: Horizontal use case

Lorraine Heilman, NOAA Center for Operational Oceanographic Products and Services
Robert Heitsenrether - NOAA Center for Operational Oceanographic Products and Services
Shaena Rausch - NOAA Center for Operational Oceanographic Products and Services
Edward Roggenstein - NOAA Center for Operational Oceanographic Products and Services
Evan Price, Nortek USA

Keywords: ADCP, currents, NOAA, horizontal

The National Oceanic and Atmospheric Administration's (NOAA) Center for Operational Oceanographic Products and Services (CO-OPS) collects high-quality nearshore currents data in both real-time and self-contained applications. The 39 CO-OPS maintained Physical Oceanographic Real-Time System (PORTS®) observatories throughout the United States coastal regions provide critical real-time oceanographic and meteorological information. The National Current Observation Program (NCOP) collects data in specific regions chosen for their relevance to navigation and commerce needs. CO-OPS current data from these programs play a key role in supporting safe navigation through real-time data and derived products such as the United States tidal current predictions. In addition, these systems provide data for a number of oceanographic research and coastal engineering applications including improving oceanographic models. CO-OPS' ability to provide versatile, accurate, and technologically up to date systems for these measurements is imperative to maintaining and enhancing these data products.

All PORTS® and NCOP measurement systems presently in operation employ acoustic Doppler current profiling (ADCP) sensors. Stations cover a variety of design types depending on site specific features and project requirements, relying on both vertically profiling, three-dimensional (3D) ADCPs and horizontally oriented, 2D ADCPs. These 2D sensors are an increasingly important component of CO-OPS' systems. A 2D horizontal ADCP system configuration allows for the sensor to be installed on a coastline structure, aid-to-navigation, or other offshore structure, and to measure currents at the channel center from a safe distance.

To increase instrument versatility, CO-OPS was motivated to test and evaluate the possibility of using a 4 beam, 3D ADCP as a 'hybrid' sensor, for either 3D vertical profiling or 2D horizontal profiling applications. This provides a strategic advantage for CO-OPS as one sensor can be used to fit a variety of applications.

The sensor chosen for this test and evaluation effort is a 250 kHz, 4 beam Nortek Signature ADCP (Signature). The lower 250 kHz frequency allows for profiles of 200 m or more, ideal for a horizontal application across a channel or vertical applications in deeper coastal waters in Alaska and other locations. Working with CO-OPS requirements, Nortek implemented a unique capability to configure the sensor to operate in either a 4 beam (3D) mode or a 2 beam (2D) mode using software controls only (no hardware modifications required). Software settings also control the sensor orientation details and other aspects of conversion from raw beam to XYZ or earth-based coordinate systems.

Figure : Test deployment showing a 250 kHz 4 beam Nortek Signature mounted horizontally.

The field site selected for the testing is at the U.S. Army Corps of Engineers Marine Traffic Control center at Chesapeake City, MD, along the C&D canal. The site is home to several operational PORTS stations, including a nearby real-time currents station that employs a Sontek 2D 250 kHz acoustic Doppler profiler (PORTS® station cb1301). The region routinely experiences regular, tidally driven currents greater than 1.5 m/s.
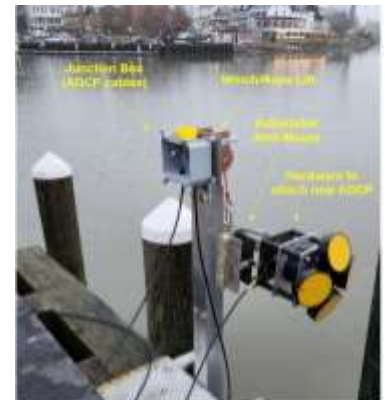
CO-OPS completed initial system integration and then deployed the system on a bulkhead structure along the canal for an extended field test starting in December 2022. The installed Signature measures horizontally across the main shipping lane at a site approximately 0.8 km eastward from PORTS station cb1301. Water depth at the deployment site is approximately 3.5 m. The channel center is approximately 100 m from the Signature with a water depth of approximately 15 m. A major challenge at this location is the relatively shallow water depth at the deployment site. Optimizing the ADCP's vertical position to ensure the greatest possible range while mitigating potential acoustic side lobe interference with sea surface and bottom boundaries requires the ability to make both vertical and horizontal adjustments to the instrument's position. For this purpose, the sensor was mounted on a vertical I-beam with a vertically and horizontally adjustable sled (Figure 1).
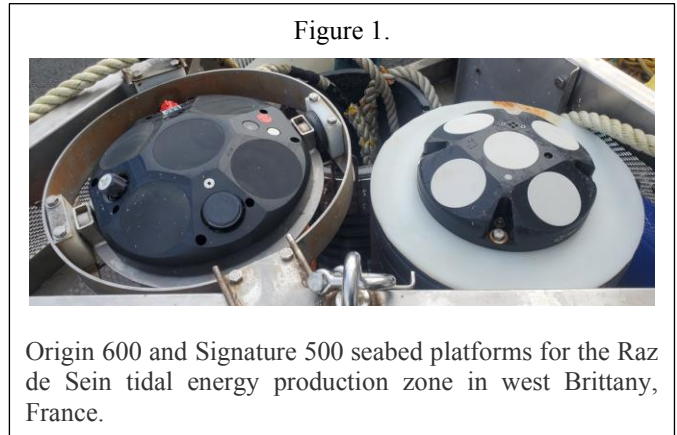
We present details associated with the Signature ADCP sensor configuration used for either 2D and 3D applications along with CO-OPS approach to system integration with real-time field systems. Changes and improvements following adjustments to the test sensors position show the sensitivity of system performance to sensor position. ADCP field test results include a comparison to transects collected with a vessel mounted ADCP system and comparisons with the existing PORTS® sensor at station cb1301, showing the improvement in data quality with the new system. Finally, next steps for system integration and operational use in PORTS® and NCOP projects will be discussed.

Currents, waves and TKE measurement for tidal-stream development using 5-beam ADCPs

Michelle Barnett, Sonardyne International Limited
Eloi Droniou, DynamOcean SARL
Marion Huchet, DynamOcean SARL
Thomas Comerford, Sonardyne International Limited
Thomas Culverhouse, Sonardyne International Limited

Keywords: Acoustic Doppler Current Profiler (ADCP), Origin 600, Signature 500, Waves, Turbulence Kinetic Energy (TKE)

Extended Abstract — Around the world, bold 'net zero' targets have been set and therefore the race is on to support this net zero transition. Offshore renewable energies are leading the charge, and environmental monitoring is a fundamental requirement for their development. Key parameters that are routinely measured include currents, waves and turbulence. Data on these ocean parameters is not only important for regulatory and legal compliance, but also for resource analysis, and making informed decisions for optimisation of energy installation design, construction planning and management. A solution for measuring all three of these parameters is the Acoustic Doppler Current Profiler (ADCP). For a three-dimensional water current profile, a 3-beam ADCP is the minimum requirement, but for advanced measurement of surface waves and for turbulence parameters such as turbulence kinetic energy (TKE), a 5-beam instrument is needed (Droniou et al., 2019). As such, 5-beam ADCPs are increasingly being deployed as assessment tools at sites with strong renewable energy potential.

Figure 1.

Origin 600 and Signature 500 seabed platforms for the Raz de Sein tidal energy production zone in west Brittany, France.

In this talk, we present the analysis of two waves and turbulence measurements datasets, which were collected at the same time and location from two different seabed-mounted 5-beam ADCPs. This analysis is a collaborative effort between Sonardyne and DynamOcean. Data comes from a recently launched measurement campaign, as part of a bid to drive tidal array development within western Brittany, France, a location with great potential for tidal stream energy. This campaign saw ADCPs deployed in the strongest tidal streams of the area to finely determine the hydrokinetic resource potential for previously identified areas of interest. One of these areas was the Raz de Sein, where two seabed mounted 5-beam ADCPs were deployed (Fig. 1). These ADCPs, a Nortek Signature 500 and a Sonardyne Origin 600, are demonstrated to measure currents, waves and TKE at the Raz de Sein tidal energy production zone over a duration of one month, inclusive of strong spring tides and especially weak neap tides. The quality of data is analysed for both the Signature

Figure 2.

Example NMEA-format output from the Sonardyne Edge Waves app.

500 and Origin 600, including PD0 format and Sonardyne's proprietary B-gram format. Waves and TKE results are compared between the two independent and different ADCPs, to bring some insight on the uncertainties of ADCP measurements and associated analyses.
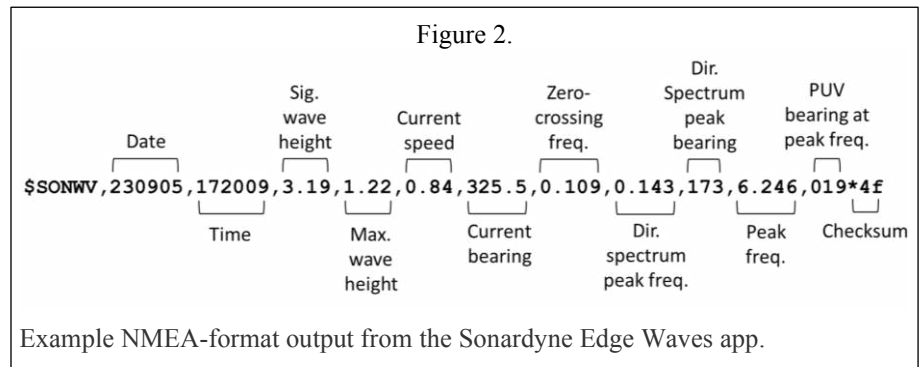
We also show how the Origin 600 ADCP successfully delivered near real-time insight into the current and wave environment at Raz de Sein (e.g. Fig. 2), and discuss the comparison between data Edge-processed during deployment and raw data processed post deployment. The interest of these new features is discussed when applied to tidal energy resource and power performance assessments within the framework of IEC's TC114 relevant technical specifications (TS 62600-200 and -201). Further details on the site, instrumentation deployment, data collection, data analysis and application are also included.

References:

- E. Droniou, M. Folley, Y. Perignon and C. Boake, "Advanced measurement and analysis of waves and turbulence using 5-, 7- or 8-beam ADCPs", *Proceedings of the 13th European Eave and Tidal Energy Conference*, Naples, Italy, 2019, pp. 1574-1 – 1574-10.

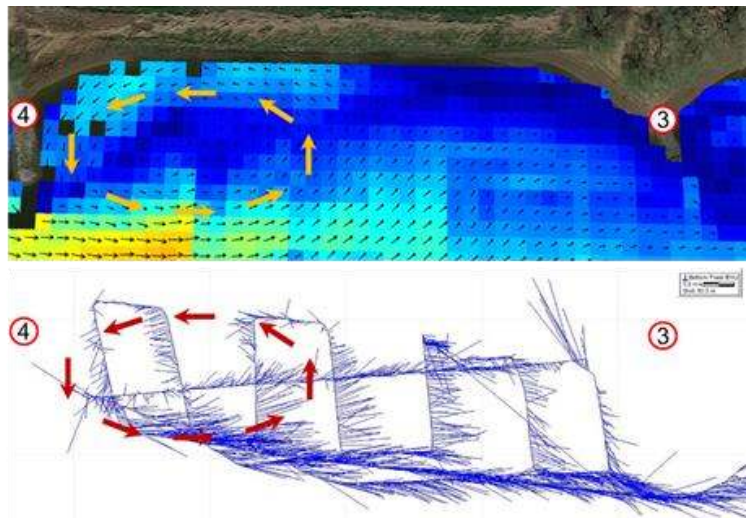# High Resolution Current Maps Retrieved from Drone Based Video

Jochen Horstmann, Marius Cysewski, Ruben Carrasco, Helmholtz-Zentrum Hereon, Germany
Thomas Lanne, Institut Polytechnique de Paris, France

Extended Abstract— High resolution surface current fields measured in space and time are of major importance for coastal engineering in particular within rivers and harbors as well as in coastal regions. Often currents induce strong morphological changes and can lead to major problems and costs in engineering projects. Detailed maps of surface currents with high spatial and temporal resolution are extremely helpful for the planning and execution of engineering tasks. Achievements of current measurements with sufficient spatial and temporal resolution is an extremely challenging and expensive task. Typically, these measurements are obtained by boat mounted Acoustic Doppler Current Profiler (ADCP) and require a lot of time and labor and typically do not allow to resolve high-resolution current fields in space and time. In the last decade marine radars (microwave radars) have often been utilized to measure surface currents. However, due to the methodology and limited resolution of the radars, these methods can only be applied in the presence of waves that are typically longer than 15 m, which often constitutes a drawback, e.g. in inlets, harbors, and rivers as well as under low wind and wave situations.

Within this study we will introduce CopterCurrents, which is a very cost-effective method to acquire surface current maps utilizing 30 s long video image sequences of the water surface waves. The video data are recorded in the range of visible light by an off the shelf drone [Stresser et al., 2017]. CopterCurrents is based on the analysis of video images for surface wave properties with respect to their wavelength as well as propagation direction and speed, which allow to extract the surface currents using the dispersion relation of ocean waves. The methodology has also been used very successfully for marine radar image sequences.

We will show several measurements obtained with Copter-Currents in different environments under various conditions, showing the applicability as well as some limitations of the method. Furthermore, we will present the results of a validation experiment performed in the tidal influenced estuary within a 100 m x 1500 m long area along the coastline of the Elbe River (Figure 1). Within this study all video sequences for CopterCurrents were acquired by an off the shelf quadcopter with an ultra-high definition (4069x2160 pixel) video camera operating with a frame rate of 25 Hz. The camera was operated at nadir (down looking) and its stabilization was performed by its active 3-axis gimbal, which very successfully compensates pitch, roll and yaw movements of the aircraft. In addition, measurements were collected by a small autonomous surface vehicle (ASV). The ASV was equipped with an RTK GPS system and a Sontek M9 ADCP. All measurements were obtained at a speed of 1 m/s over ground with the first valid bin being 17 cm below the water surface. During the entire experiment the currents were fairly homogenous over the water column and for

Current field (approx. 100m x 250m) resulting from CopterCurrents (upper panel) in comparison to current retrieved from the ADCP data aboard the small autonomous surface vehicle (bottom panel).

comparison to the drone data the ADCP data were averaged over the water column between 17 cm below the surface and 8% of the water depth above the bottom. Within the validation experiment, data were collected over an entire tidal cycle with currents speeds varying between 0 and 1 m/s and complex structures such as eddies induced by the groins. For comparison all data were co-located within 4 m of the center location of every grid cell in the drone retrieved surface current maps as well as within 7 minutes of each video recording. The comparison showed an excellent correlation (0.95), a root mean square error of 0.06 m/s with a bias of -0.01 m/s. In contrast to the ADCP data, the drone data can be obtained over a spatial large area within a very short time, and a large area can be observed with a high temporal resolution of up to 30 s, allowing to capture small spatial as well as temporal changes simultaneously. The drone measurements can also be obtained over hazardous areas, such as in front of a weir as well as in very shallow water regions.

References: Streßer, M., R. Carrasco and J. Horstmann, Video-Based Estimation of Surface Currents Using a Low-Cost Quadcopter, in IEEE Geoscience and Remote Sensing Letters, vol. PP, no. 99, pp. 1-5., doi: 10.1109/LGRS.2017.2749120, 2017.

Waves, Currents, and Suspended Sediment Measurements around Hybrid Nature-Based Solutions

Navid Tahvildari [1], Ali Shahabi [1], Andre De Souza De Lima [2], Tyler Miesse [2], Celso Ferreira [2]

(1) Department of Civil and Environmental Engineering, Old Dominion University, Norfolk, VA

(2) Department of Civil, Environmental, and Infrastructure Engineering, Geroge Mason University, Fairfax, VA

Keywords: Waves, currents, suspended sediment concentration, spectral analysis

Extended Abstract- Hybrid nature-based solutions (NbS) are constructed features that bring together natural and structural elements to attenuate wave energy while providing habitat functions. A major purpose of hybrid NbS is to address shoreline erosion which depends on wave activity and tidal currents. NbS have been the subject of many studies in recent years, but their efficiency is still not well quantified. Assessing the hydrodynamics of the flow around NbS enables a better understanding of how they affect nearshore circulation, support vegetation, and ultimately reduce erosion by preserving sediments. In this study, we measured waves, current and suspended sediment concentration (SSC) around a low-crested breakwater (or sill) and a fringing planted marsh behind it, and also measured waves around oyster bags installed in the vicinity of the first feature. The site is located in a rural area in Gloucester County in southeast Virginia. Figure 1 shows an aerial photo of the study site with the location of the instruments and Table 1 show the type of instrument(s) deployed at each location. We used high-frequency pressure sensors to measure waves on the riverside and shoreside of the sill, in the gap between two sills, and at the back of the planted marsh, behind the sill and along the gap. Wave sensors we also deployed on the river side and shoreside of oyster bags. A spectral analysis, similar to Leone and Tahvildari (2023) is conducted to quantify dissipation of spectral significant wave height as well as energy dissipation across the wave spectrum. Additionally, we deployed acoustic Doppler current profilers (ADCP) to measure incoming waves and currents in the riverside of the sill, within the marsh, and in the gap between the two sills. An ADCP was deployed offshore of the study site to measure incoming directional wave spectra for a subsequent modeling effort. To assess how the marsh-sill in the study area is reducing erosion, in addition to hydrodynamic measurements, we measured suspended sediment concentration (SSC) on the riverside and shoreside of the sill. Preliminary results show that both waves and current are attenuated by both marsh-sill and waves are attenuated by oyster bags. The field experiments started in July 2023 and will continue into spring of 2024.

Table 1. Location of the instruments and the instrument(s) deployed at each location.

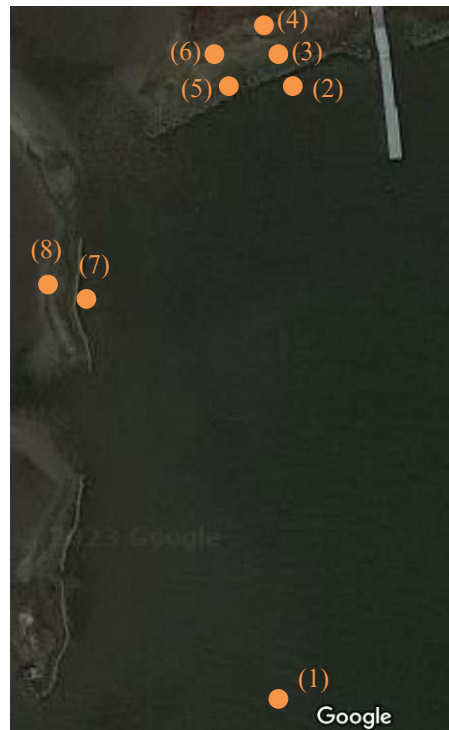| Location	Instruments
1	ADCP, Wave Sensor
2	ADCP, Wave Sensor, Turbidity Sensor
3	ADCP, Wave Sensor, Turbidity Sensor
4	Wave Sensor
5	ADCP, Wave Sensor
6	Wave Sensor
7	Wave Sensor
8	Wave Sensor

Figure 1. The layout of the instruments offshore of the NbSs (1) around the marsh-sill (2-6) and oyster bag (7,8) features (map source: Google maps)

References

Leone, A. and N. Tahvildari (2023). "Comparison of Spectral Wave Dissipation by Two Living Shoreline Features in a Sheltered Tidal Bay." Estuaries and Coasts **46**(2): 323-335.

'Wireless Waves' 20 Years On

Michelle Barnett, Sonardyne International Limited
Rick Cole, RDSEA International, Inc.
Neil Trenaman, AUUSV Inc.
Thomas Culverhouse, Sonardyne International Limited

Extended Abstract— The Ocean Circulation Group at the University of South Florida (USF) maintains a real-time monitoring program on the eastern Gulf of Mexico's west Florida shelf as part of the Coastal Ocean Monitoring and Prediction System (COMPS). Offshore data collection centers around an array of surface buoys and bottom mounted instruments for parameters including currents, temperature, salinity, and surface meteorology. 20-years ago, the need for real-time wave measurements as part of this monitoring program was recognized, the result of which was published in the paper; 'Wireless Waves' (Cole et al., 2005).

To achieve 'wireless waves' a system combining a 600 kHz RDI Workhorse Acoustic Doppler Current Profiler (ADCP) with Waves Technology, and NEMO (RDI's real-time waves processing module), acoustically connected to the surface using a set of Benthos acoustic modems, and telemetered to USF by a FreeWave radio for real-time web publishing was designed (Fig.1). The system was deployed for 17-days, producing directional wave data in near real-time. The deployment was very much the 'birth' of wireless waves technology.

Today, ADCP technology has advanced, most recently by Sonardyne International with their Origin 600 ADCP, which is an 'all-in-one' unit ADCP with integrated modem and compatibility with the Sonardyne Edge computing environment. Individually, the integrated modem presents several operational advantages, starting with removing the cost and risk of modem integration, but paired with onboard Edge data processing is where the power lies for near real-time monitoring and communications of actionable information from the seabed to the surface. The Edge data processing capability works to customize and optimize data to specific user requirements via upload of a data processing application or 'app', and Sonardyne have developed a series of core Edge apps that cater to some typical ADCP use cases. One of those use cases is waves measurements, and the Waves app has been designed for just that – to calculate a variety of wave metrics, including wave heights, periods and directional spectra, outputting as a NMEA-format string inclusive of background currents information. The Waves Edge algorithm combines the measurement of the acoustic reflection from

Figure 1.

Conceptual view of the real-time data flow from the ADCP to shore for the original 2004 'Wireless Waves' deployment (Cole et al., 2005). The new system with Origin 600 removes the requirement for intermediary kit between the ADCP and the surface buoy.

the water's surface with the water velocities from all five beams of the Origin 600 to determine the surface height and motion for each ping. From these data points, the various properties of the wave environment can be determined. The Edge app stores a buffer of data (a 20-minute ensemble) to ensure good coverage of even the longest-period waves.

An opportunity, therefore, arose and this was to demonstrate the enhanced and streamlined capability of Origin 600 for wireless waves in near real-time. We present on a comparative and collaborative effort between Sonardyne and authors of the original 'Wireless Waves' paper for achieving this offshore of St. Pete Beach, Florida, as was done for the deployment 20-years ago. The system comprised of a Sonardyne Origin 600 ADCP running the Sonardyne Waves Edge app and integrated with a turbidity sensor, exporting processed waves, currents and turbidity data to the surface via Origin 600's integrated acoustic modem, and telemetered with a cellular modem module for real-time web publishing. We show how the Sonardyne Origin ADCP's new mode of operation successfully delivered key insights on the currents and wave environment at St. Pete Beach, and we discuss the comparison between this recent deployment and the original 'Wireless Waves' deployment 20-years ago. Further details on the site, system components and data collection are also included.

References:

R. Cole, N. Trenaman, R. Weisberg and K. Amundsen, "COMPS, SEACOOS and near-shore waves," Proceedings of OCEANS 2005 MTS/IEEE, Washington, DC, USA, 2005, pp. 2415-2421 Vol. 3, doi: 10.1109/OCEANS.2005.1640128.
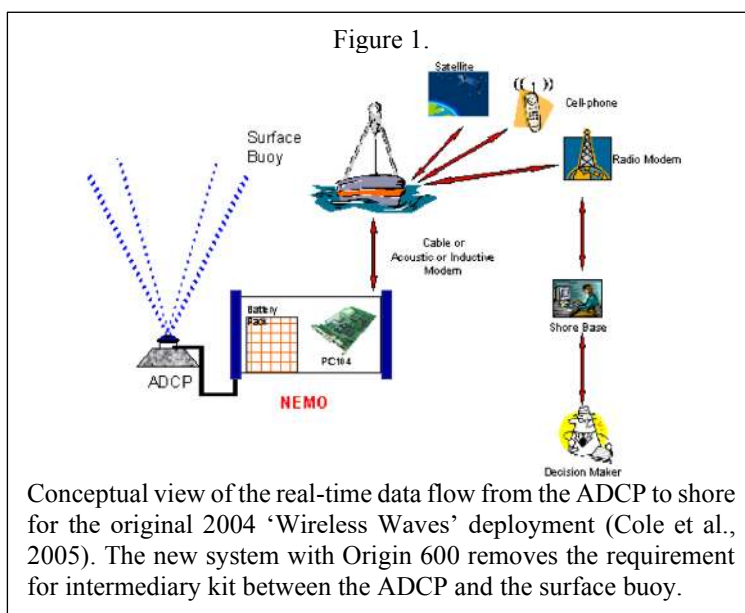
Multiscale measurements of hurricane waves using buoys and airborne radar

Jacob R. Davis, University of Washington Applied Physics Laboratory, Seattle, WA, USA
Jim Thomson, University of Washington Applied Physics Laboratory, Seattle, WA, USA
Brian Butterworth, NOAA Physical Sciences Laboratory, Boulder, CO, USA
Isabel Houghton, Sofar Ocean, San Francisco, CA, USA
Chris Fairall, NOAA Physical Sciences Laboratory, Boulder, CO, USA
Elizabeth J. Thompson, NOAA Physical Sciences Laboratory, Boulder, CO, USA
Gijs de Boer, NOAA Physical Sciences Laboratory, Boulder, CO, USA

Keywords: waves, buoys, radar, data fusion, hurricanes

Extended Abstract—The processes important to hurricane wave generation cover scales from kilometers to centimeters. Within a storm, waves have complex spatial variations that are sensitive to hurricane size, speed, and orientation. This makes it challenging to measure the spatial variability of hurricane waves with any one instrument. To obtain both broad spatial coverage and resolve the full range of wave scales, we combine arrays of drifting wave buoys with airborne radar altimetry. The microSWIFT (UW-APL) and Spotter (Sofar) buoys are air-deployed along a given storm track. These buoys resolve the scalar wave frequency spectrum from 0.05 Hz to 0.5 Hz, which is approximately 600 m to 6 m wavelength (in deep water). The Wide Swath Radar Altimeter (WSRA) flies into hurricanes aboard the NOAA Hurricane Hunter P-3s. The radar altimetry data is processed to produce a 2D directional spectrum from 2.5 km to 80 m wavelength, and the radar backscatter provides an estimate of the mean square slope from centimeter wavelengths. We use colocated observations from each instrument to create composite wave spectra with a larger range of wavelengths and better spatial coverage of observations (Figure 1). In a related approach, we explore the use of the fully 2D spectra from the WSRA with the quasi-2D directional estimates from buoys (e.g., estimates from the first five spectra moments). We also explore the dependence of mean square slope, which is a proxy for surface roughness, by combining the buoy slopes (meters) with the WRSA slopes (centimeters). Together, the fusion of these wave instruments provides a multiscale view of the hurricane-generated waves. These ocean surface waves are critical as drivers of the air-sea coupling that controls storm evolution and as drivers of coastal impacts by hurricanes.
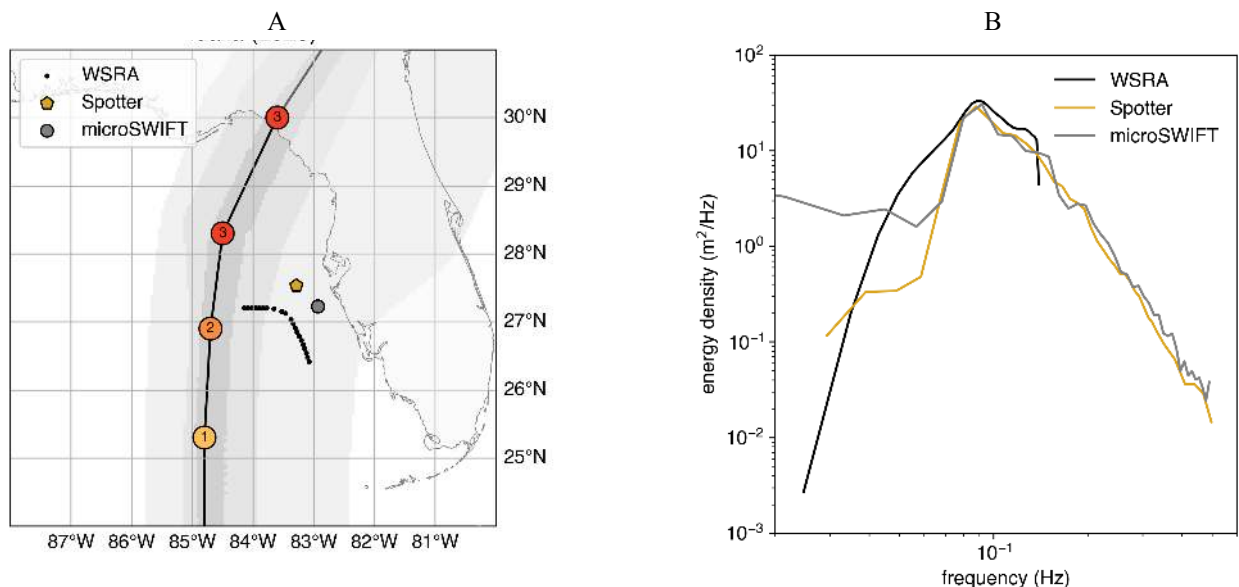
Figure 1: (A) WSRA, Spotter, and microSWIFT observations ahead of Hurricane Idalia's landfall in Florida. Points along Idalia's track are numbered by category on the Saffir-Simpson scale. (B) Scalar (omnidirectional) spectra from the three platforms sought to be combined to obtain a best estimate of the spectrum.

The Next Wave: Buoy Arrays for Deterministic Wave Prediction in Real-time

J. Thomson, Univ. of Washington, Applied Physics Lab.
A. Fisher, Washington State, Dept. of Ecology
C. Rusch, Univ. of Washington, Applied Physics Lab.

Keywords: ocean surface waves, wave prediction, real-time control

Extended abstract: Following recent work demonstrating the linear reconstruction of the sea surface from sparse arrays of wave buoys (Fisher et al 2021), we describe a system to provide deterministic wave predictions in real-time. The method uses sparse arrays of SWIFT buoys (Thomson, 2012) to form a linear propagation matrix of amplitudes and phases at discrete vector wavenumbers (Connell et al, 2015). The solution is constrained to match the conventional "first five" spectral moments reported by the buoys from the previous burst of raw data. The propagator matrix can then be used to predict the superposition of all wave components at a future time and position, though only within horizons of a few wave periods and wavelengths. Relative to a conventional statistical forecasting with random waves, the method achieves 60% improvement in prescribing the next several waves arriving at a given target location (Fisher et al 2021).

We describe efforts to make this framework operational, as shown in the figure. Radio modems to transmit raw motion data (5 Hz sampling) from the buoy array to a central node with onboard processing. The node receives the raw data and updates the propagator matrix with latency less than 1 second running on a single-board-computer (i.e., RaspberryPi). The deterministic wave prediction for a target location is then provided with a 30 seconds time horizon that is continually updated. An uncertainty metric is included in the prediction. The overall architecture is ethernet based, so integration on a wide variety of platforms. Applications include feed-forward control for Wave Energy Convertors (WECs), offshore floating wind turbines, and ship-to-ship transfers at sea. Demonstrations with the TigerRAY WEC and the WindFloat platform have recently been completed. We refer to our method as "The Next Wave" and provide public code at https://github.com/SASlabgroup/TheNextWave
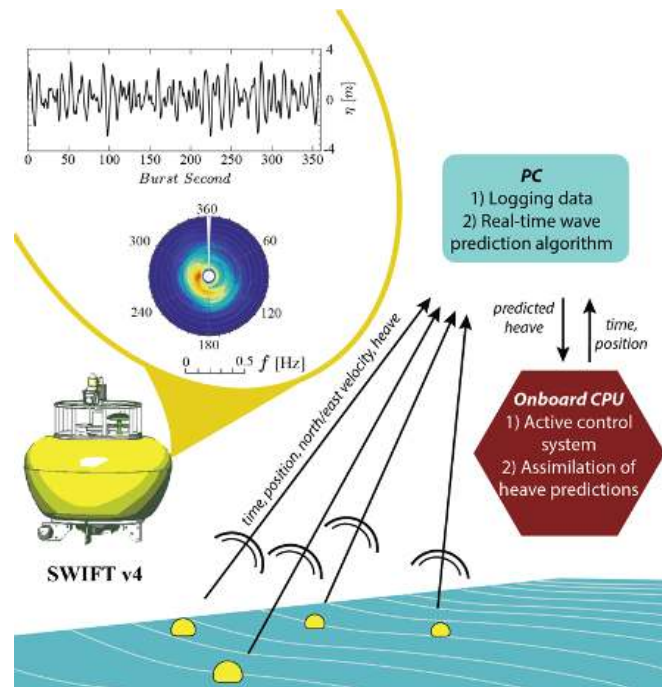
References

- Connell, B.S., Rudzinsky, J.P., Brundick, C.S., Milewski, W.M., Kusters, J.G., Farquharson, G., 2015. Development of an environmental and ship motion forecasting system. In: International Conference on Offshore Mechanics and Arctic Engineering, vol. 56598. American Society of Mechanical Engineers, p. V011T12A058.
- Fisher, A., J. Thomson, M. Schwendeman, 2021. Rapid deterministic wave prediction using a sparse array of buoys, Ocean Engineering, 228, https://doi.org/10.1016/j.oceaneng.2021.108871
- Thomson, J., 2012. Wave dissipation observed with SWIFT drifters. Journal of Atmospheric and Oceanic Technology, https://doi.org/10.1175/JTECH-D-12-00018.1

Hurricane Effects on South Florida Sea Level

William E. Baxley, FAU SNMREC

Gary A. Zarillo, Florida Inst. Technology

Keywords: hurricane, ADCP, sea level, Ekman, Coriolis, geostrophic flow

Extended Abstract—Acoustic Doppler Current Profiler (ADCP) measurements of the Florida Current (FC) offshore South Florida have been made since 2008 by Florida Atlantic University's (FAU) Southeast National Marine Renewable Energy Center (SNMREC) in Fort Pierce, Florida. The initial objective was to determine the character and energy potential of the flow in support of marine hydrokinetic energy (MHK) extraction. Recent analysis of FC ADCP data during two major hurricanes, Sandy in 2012 and Irma in 2017, have provided interesting results suggesting a connection between FC flow and temporary local sea levels during the storms. Researchers at Florida Institute of Technology (FIT) in Melbourne, Florida analyzed seasonal sea level and FC variations using sea cable voltage measurements following two hurricanes in 2022. Hurricanes Ian and Nicole provided additional indications of temporary sea level increases associated with corresponding reductions in FC velocities.

SNMREC periodically deploys ADCPs within the FC, with at least two 75 kHz Teledyne RDI (TRDI) ADCPs per mission, typically on an east-west line across the Florida Strait. Since the core of the Florida Current is shifted to the west, locations are typically within 30 km of shore, in depths from 200 to 600 m. Deployments are between 9 and 12 months in duration. Different array configurations are occasionally used, such as diamond or triangular to infer rotational features and variability along its northward path. During Hurricane Irma, however, a deployment in the axis of the FC was arranged days before landfall to obtain measurements of a passing major tropical cyclone. Two SNMREC-operated CODAR stations are also used to measure corresponding surface currents within the study area, yet during most storms municipal electrical systems are shut down to protect infrastructure, which unfortunately also terminates data collection. Upgrades are in progress to remedy this situation and provide continuous CODAR data throughout storm transits along the South Florida coastline.

Data from Hurricane Sandy indicated a strong wind-driven velocity profile deflection, associated with a considerable water level rise along the South Florida coast even though the storm center was several hundred kilometers to the east. Hurricane Irma made landfall approximately 300 km southwest of the study area near Key West, and later moved along the West Florida Coast, although its wind field still affected South Florida. In both instances, substantial water level increases appear to be wind driven due to a substantial change in FC surface flow, strong Ekman forcing, and a possible reduction in local geostrophic conditions. FIT research further showed a corresponding increase in water level with a reduction in FC velocity caused by Hurricanes Ian and Nicole in late 2022, during the annual high stand of sea level. These late season storms further amplified water levels already at a higher annual average.

A deployment is planned for early 2024 consisting of five to six ADCPs, a more resilient CODAR power system, additional meteorological stations, and possibly tide gauges deployed along the coast. This array will be designed to

North Velocity Sandy 2012

North Velocity Irma 2017

FC Flow Vs Sea Level Ian and Nicole 2022

measure not only FC velocities and variability with respect to ocean energy but will provide additional data in support of research into the additional sea level increase during tropical storm transits through the region. This additional information should assist with site-specific sea-level planning given the susceptibility of certain areas in South Florida. The deployment and equipment strategies, data analysis methods, and comparison of ADCP and sea cable measurements of hurricane effects on the FC and their possible consequences will be described, along with historical efforts and a reevaluation of existing data sets.
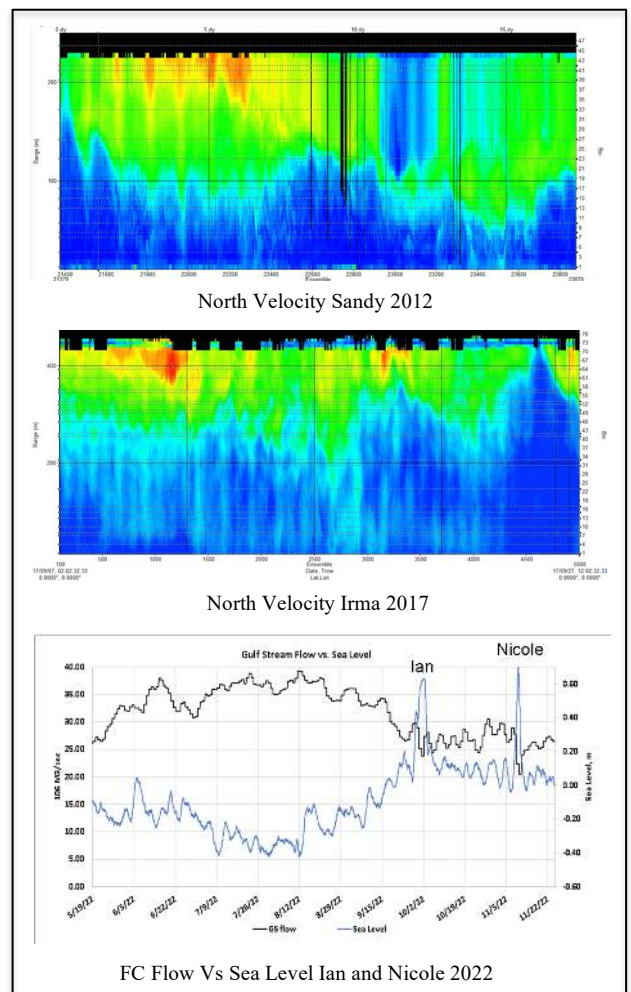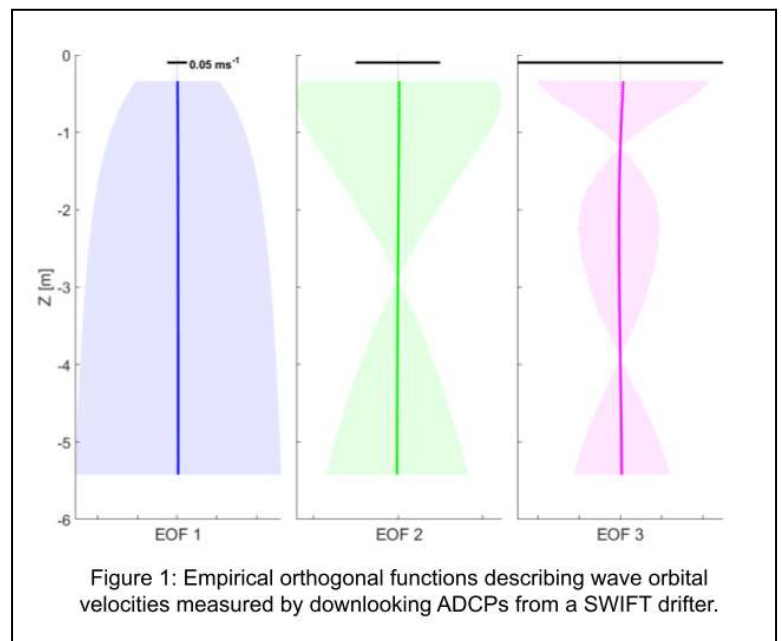
Measuring turbulence from wave-following platforms

Kristin Zeiden and Jim Thomson
University of Washington Applied Physics Laboratory

Extended Abstract —   The proliferation of Lagrangian surface platforms combined with recent improvements in acoustic Doppler current profilers (ADCPs) has enabled robust measurements of fine-scale turbulent velocities in the near surface across an increasingly wide range of forcing conditions and geographic locations. These high resolution measurements from pulse-coherent Doppler processing are ideal for estimating profiles of turbulent kinetic energy dissipation rate, $\varepsilon(z)$, using the Kolmogorov theory of inertial subrange turbulent velocity structure functions. However, strong shear associated with surface gravity waves can lead to dissipation rate estimates which are biased high (Scannell 2017). Here we present a recently developed empirical method of filtering wave orbital velocities from high-resolution ADCP data via empirical orthogonal function (EOF) analysis (Zeiden et al. 2023). The method was developed with data obtained from downlooking Nortek Signature1000 ADCPs mounted on Surface Wave Instrument Floats with Tracking (SWIFTs, Thomson 2012) and a Liquid Robotics SV3 Waveglider to produce profiles of $\varepsilon(z)$ from 0.5 - 5 meters. EOFs are well suited to capture the variance of surface gravity waves, which are coherent in (vertical) space and typically at least an order of magnitude greater than turbulent velocities (Figure 1).

We first review the results of Zeiden et. al. (2023) which demonstrate that EOFs of the data containing the most variance have characteristics of surface gravity waves, while lower energy EOFs have characteristics of inertial subrange turbulence. We then present new work to validate the inferences of Zeiden et al. (2023) by comparing the observed EOFs with those of synthetic velocity data characterized by a broadband surface gravity wave field and no turbulence. As expected, EOFs which dominate the synthetic data exhibit characteristics of surface gravity waves and closely resemble the dominant observed EOFs, while lower energy EOFs have characteristics of noise. Unlike the observed EOFs, characteristics of inertial subrange turbulence are absent from the synthetic EOFs. Finally, we expand the application of our methodology to uplooking Nortek Aquadopp-HR 2 MHz ADCPs mounted on SWIFT drifters to estimate $\varepsilon(z)$ from 0 - 1 meters. We leverage a recent data set in which SWIFTs with both downlooking and uplooking ADCPs were deployed in close proximity to produce composite profiles of $\varepsilon(z)$ from 0 - 5 meters in a wide range of seastates. The resultant dissipation rate profiles are in strong agreement with law-of-the-wall boundary layer predictions, with expected excess dissipation very close to the surface.

Figure 1: Empirical orthogonal functions describing wave orbital velocities measured by downlooking ADCPs from a SWIFT drifter.

Scannell, B. D., T. P. Rippeth, J. H. Simpson, J. A. Polton and J. E. Hopkins, 2017: Correcting surface wave bias in structure function estimates of turbulent kinetic energy dissipation rate. *Journal of Atmospheric and Oceanic Technology*, 34 (10), 2257-2273, https://doi.org/10.1175/JTECH-D-17-0059.1

Thomson, J. 2012: Wave breaking dissipation observed with SWIFT drifters. *Journal of Atmospheric and Oceanic Technology*, 29 (12), 1866-1882, https://doi.org/10.1175/JTECH-D-12-00018.1

Zeiden, K. L., J. Thomson and J. Girton, 2023: Estimating profiles of dissipation rate in the upper ocean using acoustic Doppler measurements made from surface following platforms. *Journal of Atmospheric and Oceanic Technology*, https://doi.org/10.1175/JTECH-D-23-0027.1

Validation of High-resolution ADCP Measurements of TKE Dissipation Influenced by Waves

Elias Marchetti | University of Plymouth (UK), now at University of Bath (UK)
Thomas Culverhouse | Sonardyne International Ltd.
Thomas Comerford | Sonardyne International Ltd.
Alex Nimmo-Smith | University of Plymouth (UK)

*Keywords:* Turbulent Kinetic Energy, Microstructure Profiler, Wave Energy, ADCP, Wave Orbital Velocity

Extended Abstract: This study evaluates the capability of the new Origin 600 (Sonardyne) high-resolution five-beam Acoustic Doppler Current Profiler (ADCP) to measure turbulence in shallow coastal waters influenced by surface waves. Evaluation was done through comparison between bedframe-mounted, upwards-facing ADCP data and a free-falling MicroStructure Sampler (MSS) shear probe, in turbulent flow conditions characteristic of the Tamar River channel in Plymouth Sound, UK. ADCPs are commonly used to measure water column velocity, although the low resolution of conventional units severely reduces their ability to estimate finescale turbulent motions. The new Sonardyne Origin 600 ADCP allows for much higher along-beam resolution of up to 1.2 cm, granting an unprecedented outlook into water column turbulent characteristics. ADCP-based Turbulent Kinetic Energy (TKE) dissipation estimates were computed through a second order structure function (Wiles *et al.*, 2006) for each ADCP beam, with 5, 11 and 17 radial separations and spatial velocity averaging combinations of 50, 100 and 250 bins compared to reference MSS-measured dissipation data for six measurement segments ranging from 10 to 18 minutes. Resultant radial distances, denoting the minimum observable spatial turbulence scale, ranged from 1.20 to 6.00 m for 5 radial separations, 2.64 to 13.20 m for 11 radial separations and 10.20 to 20.40 m for 17 radial separations. ADCP accuracy was computed by way of Root Mean Square Error analysis, showing a good fit between ADCP estimation and MSS reference data throughout the deployment timeline. Surface wave field conditions above the ADCP unit were also evaluated, with power spectrum density and directional analysis performed on wave heights computed from ADCP echo intensity, serving to estimate wave induced TKE dissipation contamination. While evaluation of such contamination has already been covered in other studies (Scannell *et al.*, 2017), it was performed using external buoy-based data instead of the single-source ADCP-based measurements employed in this study.

Evaluating the ADCP-based data, all binning and radial distance combinations demonstrated a good match to the reference MSS data {Figure 1A}. The higher-resolution 250-bin dataset performed best, showing the closest match throughout the majority of the water column for all radial separations. However, wave-induced dissipation was present in all ADCP datasets, Figure 1B further indicating its proportionality with proximity to the surface and larger radial separations. In addition, coherent turbulent structures caused by water column velocity shearing were also observed in the high-resolution ADCP dissipation data, more prominent shearing occurring near the surface and less discernible density-driven shearing in the midwater column.

Although further research is required to fully evaluate the accuracy of their TKE dissipation estimations, this study found that a high-resolution ADCP is a versatile tool to continuously evaluate finescale turbulence in shallow and energetic water columns, especially when compared to a lower-resolution MSS. High-resolution ADCP data can also be binned after capture, allowing for a tailored approach when measuring differing water column conditions.

Figure 1: (A) Comparison of ADCP-estimated and MSS-measured TKE dissipation for all nine binning and radial distance combinations shown in legend; (B) Estimated wave contamination in three water column sections at two radial separations shown in legend. Both subfigures utilise ADCP and MSS data from the same 12 minute deployment segment to aid compairson.

References:

Scannell, B.D. *et al.* (2017) 'Correcting Surface Wave Bias in Structure Function Estimates of Turbulent Kinetic Energy Dissipation Rate', *Journal of Atmospheric and Oceanic Technology*, 34(10), pp. 2257–2273. Available at: https://doi.org/10.1175/JTECH-D-17-0059.1.

Wiles, P.J. *et al.* (2006) 'A novel technique for measuring the rate of turbulent dissipation in the marine environment', *Geophysical Research Letters*, 33(21), p. L21608. Available at: https://doi.org/10.1029/2006GL027050.
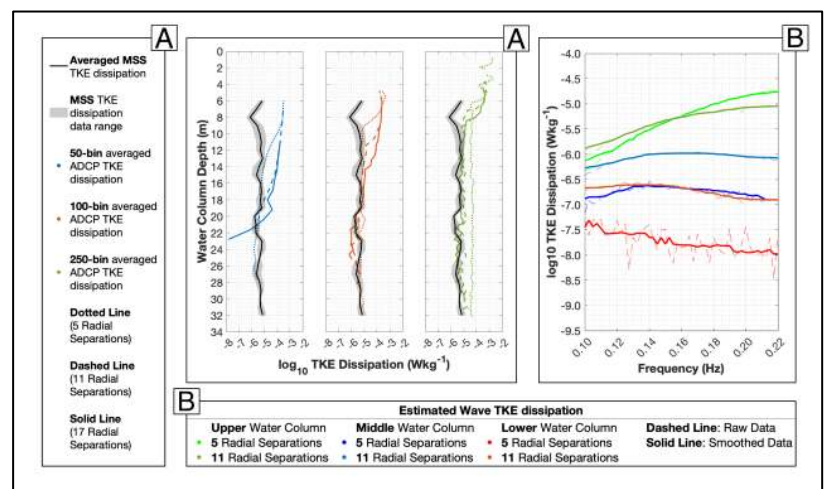
Toward a Machine Learning-Facilitated LES of Turbulent Flow Around a Solid Body

H. Ali Marefat, Scientific Computing, Faculty of Science, Memorial University of Newfoundland

Jahrul Alam, Dept. of Mathematics and Statistics, Memorial University of Newfoundland

Kevin Pope, Dept. of Mechanical Engineering, Memorial University of Newfoundland

Keywords: Subgrid-scale Model, LES, Neural Network, Convolutional Neural Network, Turbulent flow.

Extended Abstract— Machine learning- facilitated Large Eddy Simulation (LES) can significantly contribute to coastal and ocean engineering by offering refined predictive capabilities for fluid dynamics. The integration of ML with LES has the potential to advance our understanding of turbulence around solid structures, which is critical for accurate predictions in marine settings. Such enhanced simulations can lead to more precise forecasting of marine currents, wave patterns, and turbulence, facilitating better design and management of coastal infrastructure and marine navigation.

In LES, a subgrid-scale (SGS) model is used to capture the interaction between the resolved scales and unresolved ones. The Navier-Stokes equations are presented in a filtered form in LES, in which the flow motion is separated into small and large scales using a low-pass filter operation. This filtered equation consists of the SGS stress term, which provides mean dissipation that corresponds to the energy transfer from resolved scales to unresolved ones (Pope, 2000). One of the well-known SGS models is the Smagorinsky model (Smagorinsky, 1963) which uses a globally fixed value as a coefficient (known as the Smagorinsky coefficient C_s) in the procedure of approximating the mentioned dissipation. In many studies, it has been shown that a dynamically updated coefficient can improve the prediction of fluid flow in certain case studies, such as the near-wall flow. Therefore, a dynamic version of the Smagorinsky model was introduced (Germano, 1991; Lilly, 1992) in which the coefficient C_s is dynamically calculated according to the local properties of flow, obtained through minimizing Germano identity error.

In the past decade, the collected amount of data from numerical and experimental investigations in the fluid mechanics community has provided an unprecedented opportunity for implementing machine learning (ML) algorithms in computational fluid dynamics. There have been several applications of ML in fluid mechanics, such as using a deep neural network to reconstruct near-wall turbulent flow to improve the prediction of velocity field (Milano, 2002), using an artificial neural network to predict Smagorinsky coefficient for a channel flow (Sarghini, 2003), a convolutional neural network for a super-resolution reconstruction of turbulent flow (Fukami, 2019), some studies to provide an ML-based prediction for subgrid-scale stresses (Beck, 2019; Pawar, 2020).

In the current work, we employ an ML approach to obtain the Smagorinsky coefficient dynamically, using the standard dynamic Smagorinsky model framework. We have investigated a multilayer feedforward artificial neural network (ANN) in a point-wise manner and a convolutional neural network (CNN) fed by the selected snapshots of the flow. The motivation behind the current study is to address the following questions: Which data-driven methods are suitable for flow past a solid object, and which input features significantly influence the learning process using the following dataset configurations:

$$M1: \{u_i, \tau'_{ij}\} \in \mathbb{R}^9 \to \{C_s\} \in \mathbb{R}^1$$
$$M2: \{G_{ij}, \tau'_{ij}\} \in \mathbb{R}^{12} \to \{C_s\} \in \mathbb{R}^1$$

where u_i, $\tau'_{ij} = \overline{u'_i u'_j}$, and G_{ij} are velocity components, the components of resolved stress tensor, and components of the velocity gradient tensor, respectively.

In this investigation, LES of flow past a sphere at $Re = 10^3$ is considered to collect the training data. We use probability density analysis to compare the ML-based model and the dynamic Smagorinsky model. Moreover, the cross-correlation coefficient of true and predicted stresses is also presented for ANN and CNN architectures.

Density comparison of C_s for ANN (top row) and CNN (bottom row) versus dynamic Smagorinsky using dataset $M2$.

Our investigation indicates that CNN outperforms ANN, which can be due to the preservation of the multi-dimensional structure of input data. Furthermore, the dataset $M2$ shows a better prediction capability for a given ML model, suggesting that the gradient velocity tensor significantly influences the calculation of C_s.
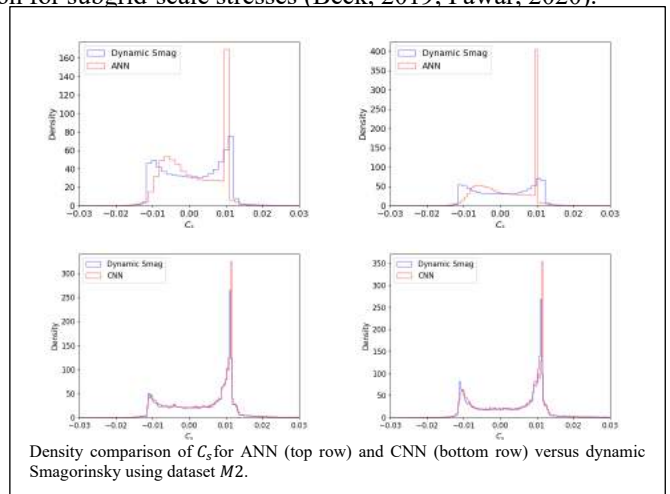
A. Beck, D. Flad, and C.-D. Munz, "Deep neural networks for data-driven LES closure models," Journal of Computational Physics, vol. 398, p. 108910, dec 2019.

K. Fukami, K. Fukagata, and K. Taira, "Super-resolution reconstruction of turbulent flows with machine learning," J. Fluid Mech., vol. 870, pp. 106–120, may 2019.

M. Germano, U. Piomelli, P. Moin, and W. H. Cabot, "A dynamic sub grid-scale eddy viscosity model," Phys. Fluids Fluid Dyn., vol. 3, March 1991.

D. K. Lilly, "A proposed modification of the germano subgrid-scale closure method," Physics of Fluids, vol. 4, 1992.

M. Milano and P. Koumoutsakos, "Neural network modeling for near wall turbulent flow," Journal of Computational Physics, vol. 182, no. 1, pp. 1–26, oct 2002.

S. Pawar, O. San, A. Rasheed, and P. Vedula, "A priori analysis on deep learning of subgrid-scale parameterizations for kraichnan turbulence," Theoretical and Computational Fluid Dynamics, 2020.

S. B. Pope, Turbulent Flows. Cambridge University Press, 2000.

F. Sarghini, G. de Felice, and S. Santini, "Neural networks based subgrid scale modeling in large eddy simulations," Computers amp; Fluids, vol. 32, no. 1, pp. 97–108, jan 2003.

J. Smagorinsky, "General circulation experiments with the primitive equations," Monthly Weather Review, vol. 91, 1963.

The Suppression of Ocean Waves by Biogenic Slicks

Nathan J. M. Laxague – University of New Hampshire
Christopher J. Zappa – Lamont-Doherty Earth Observatory of Columbia University
Shantanu Soumya – University of New Hampshire
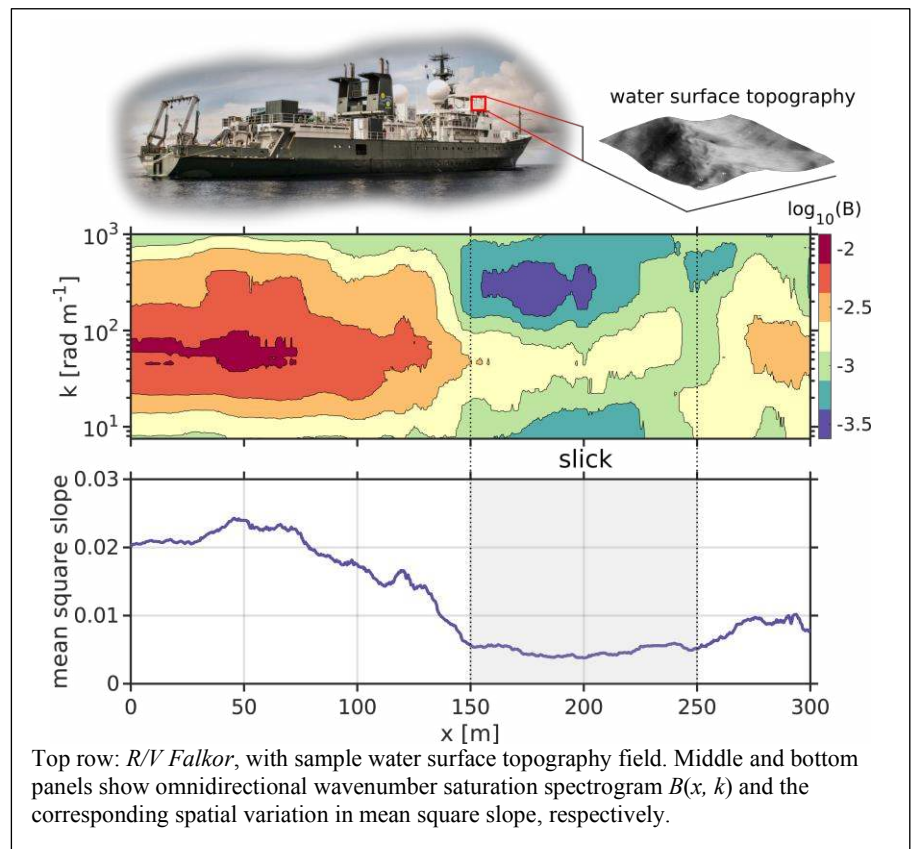Oliver Wurl – University of Oldenburg

Keywords: ocean waves, surfactants, wave damping, air-sea interaction

Extended Abstract—The exchanges of momentum, heat, and trace gases between atmosphere and ocean are critical drivers of the earth's climate. These colossal exchanges are mediated by the growth, development, and breaking of short wind-driven surface waves. Surface wave motions are significantly damped by biogenic surfactants, substances found at the ocean's surface from the high latitudes to the tropics. Consequently, the effect of surfactant compounds in the uppermost millimeters of the ocean in damping short surface waves bears greatly on earth's climatic processes. The mechanisms through which surfactants suppress waves have been studied in great detail through careful laboratory experimentation in quasi one-dimensional wave tanks. However, the spatial scales over which this damping occurs in structurally complex surfactant slicks on the real ocean have not been resolved. Here we present the results of the first-ever field observations of the spatial response of decimeter to millimeter-scale waves---the specific conduit for mediating air-sea fluxes to biogenic surfactant slicks. We found that wave damping in organic material-rich coastal waters resulted in a net (spatio-temporally averaged) reduction of ~50% in momentum input to the wave field relative to the open ocean across all wind speeds. This significant effect had thus far evaded quantification due in large part to the enormous range of scales required for its description-- spanning the sea surface microlayer to the ocean submesoscale. These results are of critical importance to describing the energy exchange between ocean and atmosphere and in forecasting the coupled earth system.

Here we present results from field observations of surface wave damping in the presence of spatially heterogeneous biogenic slicks in coastal and open ocean waters of the tropical Pacific. We resolved the spatial variation of the surface wave field for wavelengths of order 0.001-1 m over lateral lengthscales of 1 km, allowing us to determine the wavenumber-dependent damping ratio and damping coefficient. In tandem with the wave measurements, we simultaneously measured key chemical properties of the SSML (including concentration of SAS, CDOM, and chlorophyll-A) via remotely-operated

Top row: *R/V Falkor*, with sample water surface topography field. Middle and bottom panels show omnidirectional wavenumber saturation spectrogram $B(x, k)$ and the corresponding spatial variation in mean square slope, respectively.

catamaran. We found a persistent regional distinction: surface waves were weakly damped in open ocean waters, while significant damping occurred over short spatial scales in coastal waters. This distinction is owed not only to the mean concentration of surfactants in slick regions, but also to the spatial separation between individual slick filaments.

The mere presence of surfactant impacts the surface wave field and air-sea fluxes in a way that is usually not quantified (or even parameterized) in physical descriptions of air-sea interaction. Our results indicate that spatial non-uniformity in biochemical ocean surface slicks has the potential to magnify the effect of this variability, with innumerable surface roughness and temperature fields possible for any particular mean concentration of surfactant. Given the ubiquity of slicks on the surface of the coastal ocean, we anticipate that this effect is a strong (and possibly dominant) contributor to the difficulty of modeling and parameterizing air-sea interaction in nearshore zones.

Passive Infrared Sea State Sensing

Steven P Anderson, Areté
Alex Campbell, Areté

Keywords: sea state, infrared, polarimeter, stereo, waves

Extended Abstract—

Passive remote sensing of ocean waves holds the promise of providing a low-power, non-contact solution to measure sea states. Here we explore the feasibility of using a longwave infrared stereo and/or polarimetric wave-imaging camera to provide a day/night capability to observe surface slope fields and derive sea state (wave height, period, direction, and directional wave spectra). A new passive sea state sensor could be deployed on offshore structures such as oil platform and wind turbines. The system would also measure surface currents through well-established space-time processing techniques. The cameras are mounted well above the sea surface and look down and away from the platform. This configuration reduces installation and maintenance cost relative to in situ (in water) instruments and buoys and avoids wake from the platform or structure.

There has been prior work on stereo and polarimetric wave imaging to derive wave heights and directional spectra. Stereo processing techniques are well developed within the computer vision field, with numerous off-the-shelf algorithms available for the processing chain from keypoint detection and matching, image rectification, and disparity mapping. Many of these studies have employed panchromatic cameras, thus limiting the capability to daylight hours. However, an operational sea state sensor needs to operate day and night and in a range of environmental conditions. Here we explore using long-wave infrared (LWIR) stereo imaging to provide a day-night solution.

Ocean wave measurements using Structure from Polarization (SfP) has only been demonstrated on the research level and not in the LWIR band. A new state-of-the-art commercial-of-the-shelf (COTS) Pyxis Longwave Infrared Polarimetric Imager is now available. It holds the promise of enabling a day and night SfP wave sensing capability.

In April 2023, we conducted a field study at Frying Pan Tower to collect wave imagery. Panchromatic and LWIR stereo cameras and a LWIR polarimeter were mounted 25 meters above the sea surface to image waves and provide the raw data needed to develop and validate algorithms. An airgap measuring lidar was deployed to provide ground truth.

The field collection data will be used to directly demonstrate feasibility, illuminate outstanding technology risks, and provide the first reduction of our concept to practice. Here, we report on our experiences with the camera systems, share lessons learned, and provide preliminary results.
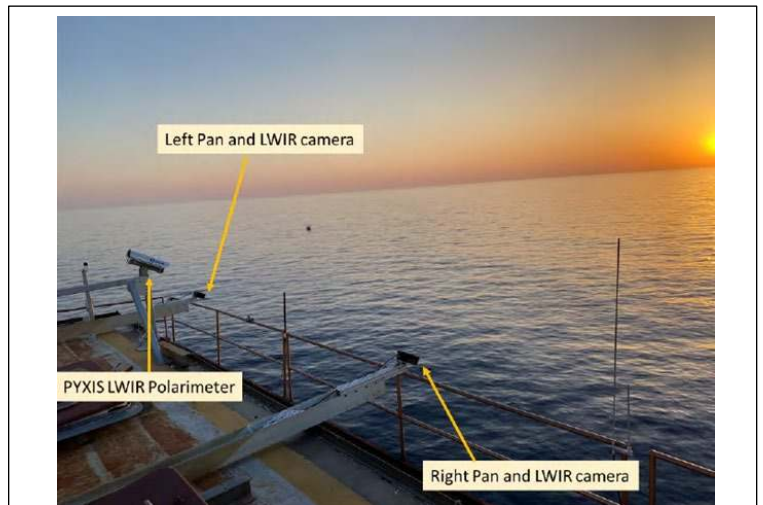

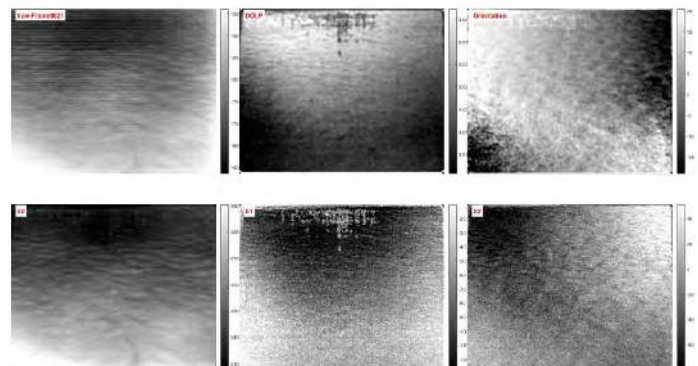Figure 1. View of the camera systems deployed at Frying Pan Tower.

Figure 2. An example of a single image from the Pyxis polarimeter. The frames show the total intensity, the Degree of Linear Polarization, the Orientation and the three Stokes components.

Coastal Oceanographic Observations off of North Carolina

Caroline Lowcher, ECU Coastal Studies Institute

Mike Muglia, ECU Coastal Studies Institute

Trip Taylor, ECU Coastal Studies Institute

Keywords: Radar, Buoy, and ADCP Observations

Abstract: Ocean observations are a critical component of the Decade of Ocean Science's objectives enhancing scientific knowledge that supports sustainable development of the ocean. We operate multiple observational platforms off of NC that measure waves and currents and these observations characterize the marine environment. Characterization of the physical ocean environment is crucial to inform the development of renewable ocean energy devices like wave energy converters (WECs), kites, and turbines. Our research group has years of observations in the Outer Banks region which includes directional wave spectra from a suite of buoys and radar, Gulf Stream observations from moorings and land-based high frequency (HF) radars, and several vessel-based measurements from our research vessel, *Miss Caroline*. Our 3 Waverider buoys deployed 10 miles off of Nags Head, Oregon Inlet, and Buxton have informed two ~40-year wave hindcasts for our region. These hindcasts provide robust estimates of the wave energy resource and its seasonal variability for WEC developers. Several years of acoustic Doppler current profiler (ADCP) measurements characterize the available current resource on the upper continental slope from the Gulf Stream off of Cape Hatteras, NC and our coastal ocean radar network identifies meander-scale and longer variability over this region. These extensive shelf and Gulf Stream observations as well as our expertise developing, deploying, and recovering observing systems in the ocean have led to several funded collaborations with developers to deploy WECs, kites, and turbines to support blue economy development. These efforts helped support establishing the Atlantic Marine Energy Center and its wave energy test site at Jennette's Pier, as well as several successful collaborations through our state funded NC Renewable Ocean Energy Program.
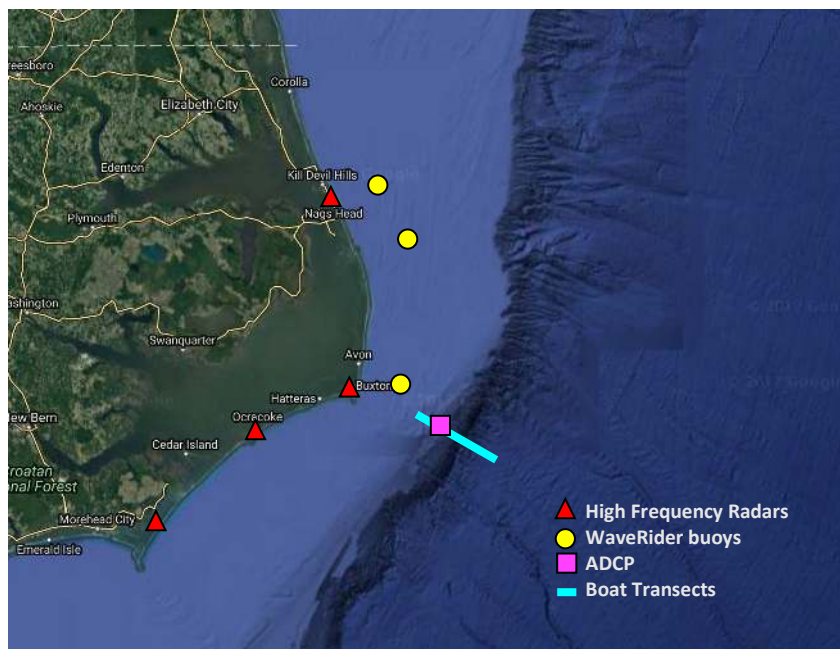
HF Radar for Sustainable Development in Coastal Waters

Thanh Huyen Tran[2,5], Mal Heron[1], Jan Widera[2], Herman Peters[3], Roberto Gomez[2], Thomas Helzel[2], and Pieter Dekker[3]

[1]James Cook University, Townsville, Australia
[2]Helzel Messtechnik GmbH, Kaltenkirchen, Germany
[3]Xi Advies B.V., Nieuw-Buinen, The Netherlands
[5] Laboratory of Oceanology and Geosciences, CNRS UMR 8187, ULCO, ULille, IRD, France

Keywords: Lagrangian, HF radar, Coastal management

Extended Abstract—Coastal oceans directly affect much of the world's population and this points to a need for management technologies for sustainable development in coastal waters. HF radar is an ideal technology for studying dynamics in the coastal oceans and there has been an emphasis on large-scale dynamics and seasonal variability. In this study we focus on the high precision capabilities of HF radar for fine-scale monitoring for water quality and buoyant pollution management in the coastal zone. The surface current data are from the WERA HF radar installed at the Port of Rotterdam and being used in real time for safe and efficient operation of the port.

Figure 1. Initial locations of parcels of surface water near high tide (left), and final locations after one tidal cycle (right). The WERA radar at Rotterdam has a larger grid and we include only those starting locations that connected to a final location without drifting outside the domain. The coastline is sketched in green.
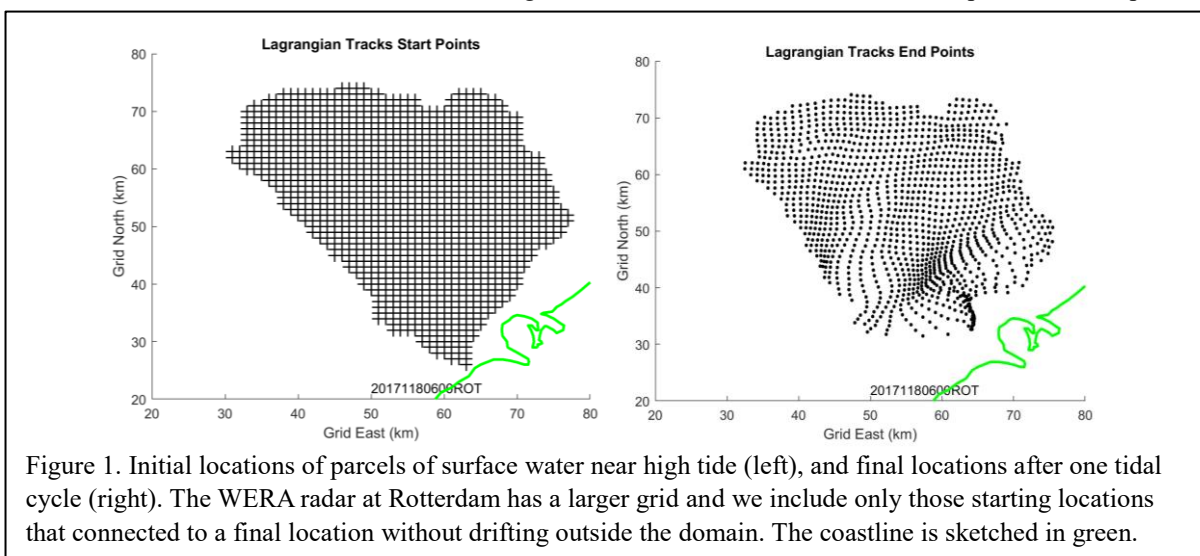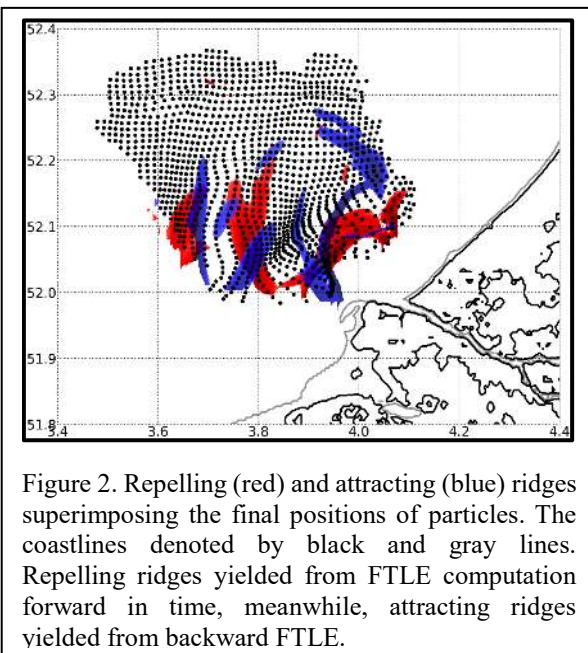
Fig. 1 shows that, a regularly-spaced grid of parcels of surface water becomes warped as time passes, with some areas of concentration and other areas of dilution on the surface. We first examine the interpretation of the separation of particle pairs in diffusion. It is clear that the concept of diffusion requires a larger domain than this and must include all scales of turbulence.

For tackling the limitation of diffusion concept, Finite-Time Lyapunov Exponent (FTLE) and Finite-Size Lyapunov Exponent (FSLE) were used for determining the concentration and dilution areas governed by Lagrangian coherent structures (LCSs) A concentration band is found in front of the river mouth where the attracting FTLE ridges (demonstrated by blue color) act like 'magnets' trapping particles. The repelling ridges (red) at the right arm of the river outlet represent the trend of particle spreading. However, the dispersion was hindered by the attracting ridges, therefore, particles could not spread farther offshore.

Figure 2. Repelling (red) and attracting (blue) ridges superimposing the final positions of particles. The coastlines denoted by black and gray lines. Repelling ridges yielded from FTLE computation forward in time, meanwhile, attracting ridges yielded from backward FTLE.

This approach will be a significant contribution to the management of water quality and pollution in sensitive coastal areas like Ports, reserves, and Marine Protected Areas.

Use of In Situ Air-Sea-Wave and Direct Covariance Flux Observations to Constrain a Model for Seastate-Dependent Sea Spray-Mediated Air-Sea Heat Fluxes in High Winds

Benjamin W. Barr, Hyodae Seo, Carol Anne Clayson, and James B. Edson
Woods Hole Oceanographic Institution, Woods Hole, MA, USA

Keywords: air-sea heat fluxes, direct covariance flux measurements, high winds, sea spray, parameterization

Extended Abstract—Air-sea fluxes of sensible and latent heat are fundamental to the energetics of tropical cyclones (TCs) and their intensity. In high winds (i.e., 10-m windspeed $U_{10} \gtrsim 20$ m s^{-1}), sea spray droplets ejected from breaking waves provide pathways for heat transfer (i.e., droplet cooling and evaporation) that are not represented in the bulk heat flux algorithms widely used in TC forecast models. Sea spray generation and heat fluxes are controlled by complex interactions at breaking wave crests and in the spray-laden atmospheric surface layer. However, co-located in situ measurements of high-wind spray generation and air-sea heat fluxes, as well as the wind, wave, and turbulent upper ocean conditions that produce them, are extremely limited. Advancement of seastate-dependent algorithms for air-sea heat fluxes with spray through improved model physics and observational constraint is an active area of research for TCs, which may also benefit the forecasting skill of other high-wind and high-flux conditions under extratropical cyclones.

Recent work has produced a new parameterization for seastate-dependent air-sea heat fluxes with spray for use in fully coupled atmosphere-wave-ocean TC forecast models (Barr et al. 2023). This parameterization predicts spray generation based on wave properties including wave energy dissipation flux and significant wave height, and it allows both the total mass of generated spray and the droplet size distribution to change with wind-wave conditions, reflecting recent laboratory findings. TC model simulations testing the new parameterization demonstrate a consistent influence of spray on TC intensity that is explainable by the physics of droplet cooling and evaporation that the parameterization represents (Barr and Chen 2024). Though an encouraging step towards improved modeling of high-wind heat fluxes in coupled air-sea-wave systems, the parameterization is considered poorly constrained due to limited available observations during its development.

In the current work, we incorporate the aforementioned spray parameterization into the Coupled Ocean-Atmosphere Response Experiment (COARE) air-sea heat flux algorithm (Edson et al. 2013) and constrain the model physics using high-wind in situ measurements of direct covariance heat fluxes and conditions at the air-sea interface. Observations come from diverse field campaigns and sites, including the CLIVAR Mode Water Dynamic Experiment (CLIMODE), the Salinity Processes in the Upper-ocean Regional Study (SPURS) 1 and 2, and multi-year measurements from the NSF Ocean Observatories Initiative (OOI) Pioneer, Endurance, and Irminger Sea Arrays. We compare the new version of the COARE algorithm with spray to earlier versions without spray and demonstrate the divergent outcomes of extrapolating the models past the observed range of U_{10}.

This work highlights the need for systematic, long-term, and simultaneous observations of winds, waves, spray, surface thermodynamics, and heat fluxes in high winds and serves as a "proof of concept" study for how these observations could be used to calibrate air-sea heat flux algorithms with spray. We discuss how existing or planned sites might be used to obtain the necessary measurements if augmented with additional systems to measure, for instance, (in order of increasing difficulty) direct covariance turbulent latent heat fluxes, ocean-side near-surface turbulent dissipation, and the generated spray droplet size distribution.

Barr, B. W. and S. S. Chen, 2024: Impacts of seastate-dependent sea spray heat fluxes on tropical cyclone structure and intensity in fully coupled atmosphere-wave-ocean model simulations. *J. Adv. Modeling Earth Syst.*, In preparation.

Barr, B. W., S. S. Chen, and C. W. Fairall, 2023: Sea-state-dependent sea spray and air-sea heat fluxes in tropical cyclones: A new parameterization for fully coupled atmosphere-wave-ocean models. *J. Atmos. Sci.*, **80**, 933 – 960, https://doi.org/10.1175/JAS-D-22-0126.1.

Edson, J. B., V. Jampana, R. A. Weller, S. P. Bigorre, A. J. Plueddemann, C. W. Fairall, S. D. Miller, L. Mahrt, D. Vickers, and H. Hersbach, 2013: On the exchange of momentum over the open ocean. J. Phys. Oceanogr., 43, 1589 – 1610, https://doi.org/10.1175/JPO-D-12-0173.1.

Determining the Origin and Fate of Oceanic eDNA

Hugh Roarty, Rutgers University
Brendan Henley, Rutgers University
Tim Stolarz, Rutgers University
Jason Adolf, Monmouth University
Josh Kohut, Rutgers University

Extended Abstract— Trawling has been the traditional method for monitoring benthic communities. Offshore wind is rapidly developing with the Mid Atlantic waters of the United States. Construction of wind turbines will pose challenges to traditional sampling methods because trawling gear in the vicinity of turbine foundations will be limited. Environmental DNA (eDNA) has emerged as a new tool for monitoring marine ecosystems and biodiversity. The use of eDNA is a cost-effective approach to replace traditional sampling.

However, there is limited information on the origin, fate and transport of eDNA in the ocean. Therefore, we utilized surface current data from a High Frequency radar network to advect particles backward in time to assess the origin of water that was sampled as part of an eDNA sampling campaign.

eDNA was sampled west of Cape May, NJ on December 8, 2021. Twenty surface particles were released in the HFR surface current field and allowed to drift backwards in time for five days (Figure 1). Surface and bottom currents from the DOPPIO regional ocean model were also used to transport the passive tracers backwards in time.

In this one instance using the HFR surface currents the particles advected to the northwest over the five days originating in the back bays of Cape May NJ. The particles travelled approximately 35 km over the five days. Similarly, the DOPPIO surface currents also indicated a reverse drift to the northwest but after 2 days the currents weakened and particles remained near the sampling location. In contrast the DOPPIO bottom currents displayed a different trajectory indicating source waters originated from the south.

These findings underscore the significance of considering various data sources and models when analyzing eDNA transport, as well as the potential for HF radar surface current data to provide valuable insights into the origin and transport of marine genetic material. The half-life of eDNA in marine environments has been estimated at approximately one day, allowing travel times determined here to be used to approximate the relative abundance of 'local' vs 'transported' eDNA at a given sampling location. Such research is crucial as the offshore wind energy industry continues to expand, emphasizing the need for innovative monitoring methods to ensure effective environmental stewardship and biodiversity conservation in the changing coastal landscape.
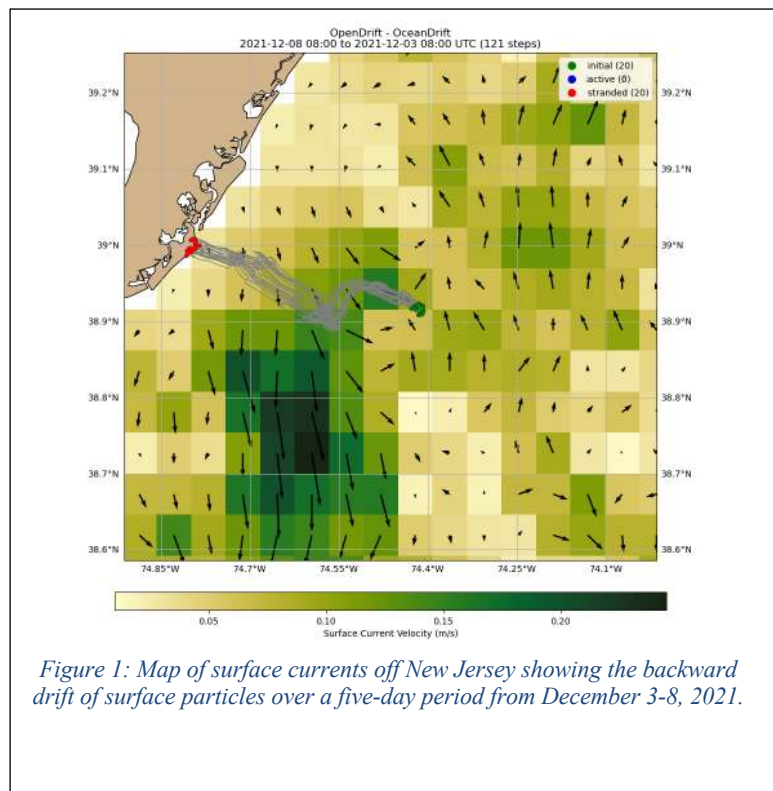

Figure 1: Map of surface currents off New Jersey showing the backward drift of surface particles over a five-day period from December 3-8, 2021.

Determining the Seasonality of Oceanic eDNA Source Waters

Authors: Brendan Henley[1], Tim Stolarz[1], Hugh Roarty[1], Jason Adolf[2], Josh Kohut[1]

Affiliation: [1]Rutgers University, [2]Monmouth University

Keywords: environmental DNA, currents, HF radar, particle tracking.

With offshore wind development planned for US coastal waters, there are potential impacts construction and operation may have on traditional surveys used to assess the marine species that live within turbine farm areas. Environmental DNA (eDNA) offers a uniquely efficient method of monitoring marine communities since species do not have to be actively caught with a traditional vessel based trawl survey. This allows for a low-cost opportunity to continue species assessment in areas inaccessible to traditional surveys. However, to properly interpret sources of the sampled eDNA, we need to better understand where the eDNA originated.

To better understand the range and movement of the ocean water containing specific eDNA samples, we utilize backwards drift current models to identify the origin of the eDNA and the dependence of source range on location and seasonality.

Using HF Radar surface current data over a 10-year data set from 2007 to 2016, we simulated the reverse drift of particles off the coast of southern NJ in offshore wind energy areas. This was done using the OpenDrift model that was seeded with 100 virtual particles going backwards for five days, encompassing the likely lifetime of eDNA in the water. This was done at three test locations of varying distances from the shore, and it is done for a starting date that is indicative of each season of the year (February, May, June, November). Both animations of particle movement and plots of distance from the starting point were generated for analysis. This analysis focused on the distance from shore and season versus the distance between eDNA sample location and source waters.

Initial analysis suggests that eDNA has the potential to travel farther in fall seasons compared to summers. Viewing animations revealed that this difference in paths of the particles was due to greater strength of currents in the fall (from storm events or higher average wind strength), while in summer, when winds are more relaxed, the particles are advected by the tides close to the origin. A more practical result of the analysis is that around the 24-hour mark, particles originated within ~10 km of sampling location regardless of season or location (24 hours is a currently respected approximation for half-life of an eDNA sample, so this time range is of particular importance to take note of). Therefore, variability in travel distance was only seen over greater time periods beyond 24 hours. This long-term variability was shown to be due to the seasonality, rather than particle release location.
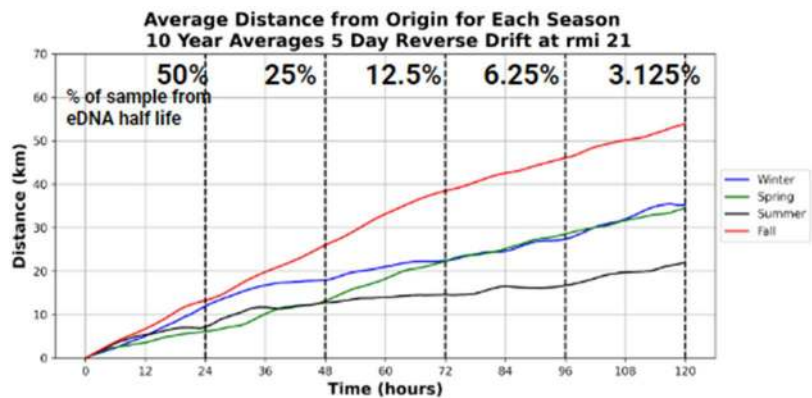

Figure 1: Averages distance traveled from origin of 100 simulated drifters in each season of the year from 2007-2016. Dotted lines at each 24 hour mark represent an approximation for the half life of an eDNA sample.

This research will provide knowledge on the distance and path that particles travel in the ocean. This will be useful by providing context for eDNA measurements and helping identify the origins of eDNA. Understanding the dependence on seasonality will improve the quality of sampling by being able to take these patterns into account. This research provides information on another factor that should be considered if fisheries managers want to leverage the full utility eDNA sampling. Since this method of sampling is currently being developed, understanding everything we can learn from eDNA samples is imperative to preserve life in the ocean.

Distributed acoustic sensing (DAS) of seafloor fiber optic cables enables meter-scale resolution of surface waves in the coastal ocean

Maddie Smith, Woods Hole Oceanographic Institution
Jim Thomson, University of Washington
Hannah Glover, Oregon State University
Meagan Wengrove, Oregon State University
Michael Baker, Sandia National Laboratories
Rob Abbott, Sandia National Laboratories
Jacob Davis, University of Washington
Seth Zippel, Oregon State University
Wenbo Wu, Woods Hole Oceanographic Institution

Extended Abstract—Distributed acoustic sensing (DAS) provides a novel opportunity to turn coastal seafloor telecommunication and other fiber optic cables into high-resolution surface wave measurement arrays. A DAS interrogator is connected to the shore end of a fiber to measure strain or strain-rate by observing the reflection of lasers off impurities in the glass. Strain or strain-rate is responsive to variations in seafloor pressure (as well as acoustic and other waveforms in the water column) allowing each channel to act like a seafloor pressure mooring. This allows a fiber up to tens of kilometers in length with channel spacing of meters to act like a series of thousands of virtual wave buoys. Thus, it provides a particularly appealing method for observing spatial and temporal changes in wave conditions in regions with high spatial gradients, such as seasonally ice-covered coastal environments.

The presence of surface wave signals have been observed in cables globally in a wide range of environments (e.g., Lindsey et al., 2019), and these signals have now been successfully used to quantify wave spectra and statistics (e.g., Smith et al., 2023, Glover et al., 2024). Here we demonstrate methods for wave retrieval from seafloor cables with DAS using observations from over 30 km of telecommunication cable in the Alaskan Arctic, over 6 km of communication cable connecting to an oceanographic tower in the coastal Atlantic (Martha's Vineyard), and 1 km of custom-installed cable at the USACE Field Research Facility in Duck, NC. Using empirical

calibrations specific to each cable, the DAS-derived wave statistics agree well with conventional in situ measurements (correlations of $R^2 > 0.8$). We summarize these diverse calibration datasets in an effort to understand and describe the controls on strain-rate response to surface waves, such that future DAS collections may need less empirical calibration. This approach provides notably higher spatial resolution of wave statistics than achievable by other in situ methods, and utilization of existing cables can require less logistical effort than in situ sampling.
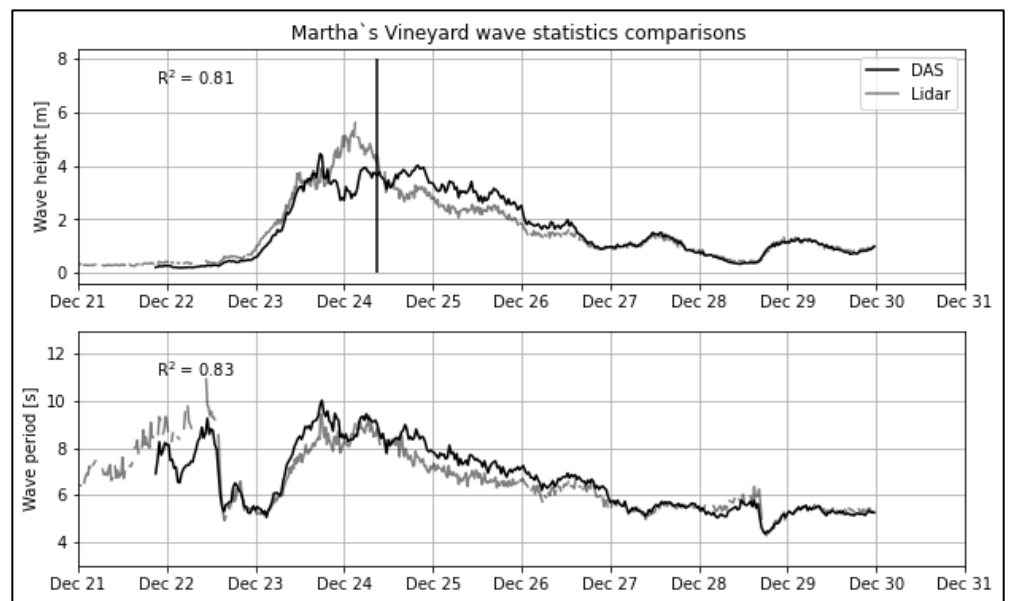
Glover, H.E., Wengrove, M.E., Holman, R. (in review) Measuring hydrodynamics and exploring nearshore processes using distributed sensing of fiber-optic cable strain. Coastal Engineering.

Lindsey, N. J., Dawe, T. C., & Ajo-Franklin, J. B. (2019). Illuminating seafloor faults and ocean dynamics with dark fiber distributed acoustic sensing. Science, 366(6469), 1103–1107. https://doi.org/10.1126/science.aay5881

Smith, M. M., Thomson, J., Baker, M. G., Abbott, R. E., & Davis, J. (2023). Observations of ocean surface wave attenuation in sea ice using seafloor cables. Geophysical Research Letters, 50, e2023GL105243. https://doi.org/10.1029/2023GL105243

Enhanced Underwater Acoustic Channel Estimation using BSMVC Method

Fei-Yun Wu, Navigation College, Jimei University, Xiamen, China
Dan Song, Navigation College, Jimei University, Xiamen, China

Extended Abstract—This study introduces a novel approach, the Block Sparsity Constraint Maximum Versoria Criterion (BSMVC) method, for precise underwater acoustic channel estimation. By leveraging block sparsity constraints and the Maximum Versoria Criterion, the proposed method optimally captures inherent patterns and correlations within signal blocks, significantly improving the accuracy of channel representation. Through extensive simulations, the BSMVC method demonstrates superior performance compared to traditional approaches, showcasing its effectiveness in handling the dynamic nature of underwater channels. This method presents a promising advancement for researchers and practitioners aiming to enhance the reliability and performance of underwater communication systems.

To improve the accuracy of channel representation, we aim to accelerate the convergence and reduce the steady-state misalignment of the traditional adaptive estimation methods [1-4]. First, we design a block sparse constraint, i.e., $l_{\infty,0}$ norm for the cluster sparse underwater acoustic channel and insert it into the cost function of the MVC algorithm. Second, the optimization iterations are obtained via maximum gradient ascent strategy. Simulations are conducted to evaluate the performance of the proposed $l_{\infty,0}$-MVC method.

This study proposes a block sparse constraint based method, i.e., $l_{\infty,0}$-MVC algorithm, to improve the estimation accuracy of the MVC method. First, we analyzed the derivations of MVC method and the relationship of metric and norm constraint. Then, we designed a block sparse constraint via $l_{\infty,0}$-norm and derived its gradient expression. The $l_{\infty,0}$-MVC algorithm is specially designed for identifying the block sparse underwater acoustic channel. Meanwhile, it can be regarded as an extension of sparse constraint version when the block size is set as 1. We provide the performance discussion including convergence and steady-state-error analysis of the proposed $l_{\infty,0}$-MVC algorithm. In simulations, we formed the problems of the identification and tracking for the block sparse underwater acoustic channel, to test the $l_{\infty,0}$-MVC algorithm and its counterparts, which are including SA, MVC, GMCC, and l_1-MVC methods. The results confirm the superior performance of the proposed $l_{\infty,0}$-MVC algorithm in terms of faster convergence and lower misalignment.

The learning curves of different methods with different block sparsity.

The simulation is designed to test the performance of the proposed $l_{\infty,0}$-MVC method with different block sparsity. For comparisons, the counterparts include SA, MVC, l_1-MVC, GMCC methods with different p settings. We test their learning curves with the unknown underwater acoustic channel of different block sparsity. We set $c = 1$, and block sparsity κ as 1, 2, 3, 4, respectively. The corresponding sparsity is then 5, 10, 15, and 20, respectively.

The results of learning curves with different block sparsity are shown as Figure. One can see that: With the same noise level, the sparse constraint algorithms including l_1-MVC and $l_{\infty,0}$-MVC methods show its superior performance in terms of estimation accuracy. However, as the increasing of the block sparsity, the accuracy of l_1-MVC method suffers dramatically. Because compared with l_1 norm constraint, the block sparsity exploitation facilitates the tolerance of different sparsity.

[1] Ben-Xue Su, Fei-Yun Wu, Kun-De Yang, Tian Tian, Yi-Yang Ni, Steady-state mean-square performance analysis of the block-sparse maximum versoria criterion, Signal Processing, 2023, 213, 109186

[2] Hu, X., Wang, Y., Wu, F., & Huang, A. A mixing regularization parameter IPNLMS for underwater acoustic MIMO channel estimation. AEU-International Journal of Electronics and Communications, 2022, 155, 154366.

[3] Tian Tian, Fei-Yun Wu, Kunde Yang, Block-sparsity regularized maximum correntropy criterion for structured-sparse system identification, Journal of the Franklin Institute, 2020,357(17): 12960-12985

[4] Fei-Yun Wu, Yan-Chong Song, Ru Peng, A Scaled LMS Algorithm for Sparse System Identification with Impulsive Interference, Circuits, Systems, and Signal Processing, 2023, 1-10
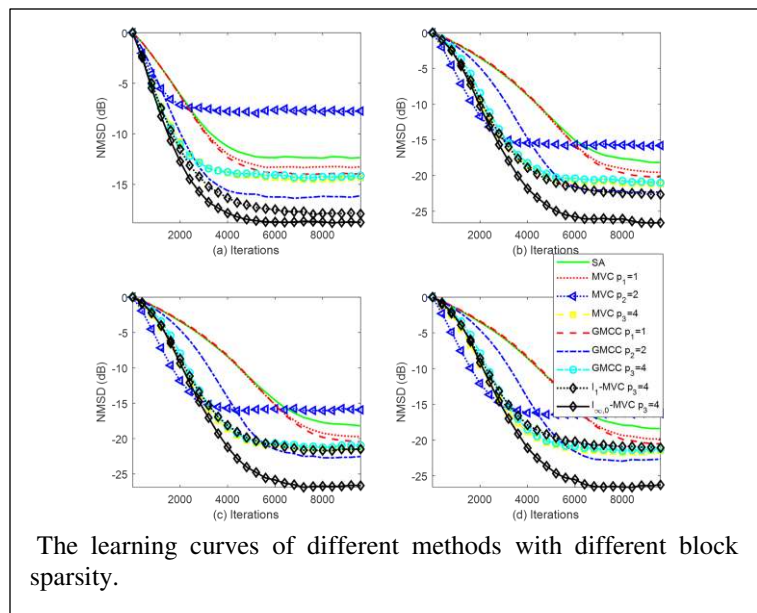
Vulnerabilities of Opportunistic Routing in Underwater Acoustic Sensor Networks

Ruiqin Zhao[1,2], Bingyu He[1]

[1]School of Marine Science and Technology, Northwestern Polytechnical University, Xi'an, China
[2]Key Laboratory of Ocean Acoustics and Sensing (Northwestern Polytechnical University),
Ministry of Industry and Information Technology, Xi'an, China

Keywords: underwater acoustic sensor networks; vulnerability; security; opportunistic routing

Extended Abstract—Underwater acoustic sensor networks (UASNs) have a wide application in marine exploitation and marine surveillance . However, due to the broadcast nature of underwater acoustic channels, transmitted packets are prone to be monitored by unauthorized sensor nodes. Moreover, the propagation delay of underwater acoustic communication is long, and the nodes generally move or drift with ocean current, which makes it is difficult to verify the true geographical location of a node [1]. Opportunistic routing (OR) mechanisms, that generally are node location-aware, have been extensively employed in UASNs for its superiority on combating the unpredictable link interruptions [2]. In this paper, we investigate the vulnerability of UASNs using OR under location spoofing attacks. We try to analyze the exposure risk of location spoofing attacks at different locations in the network, where a lower the risk of malicious attack exposure means a worse network vulnerability.

Our analysis is based on the depth based routing (DBR) [3] where packets are relayed based on node depth. r is the transmission radius for each node in the network. Malicious nodes use location spoofing to attract traffic to interfere with packet delivery, which is similar to blackhole attacks. We study two scenarios, i.e., the malicious node exists within one-hop range of the source node and in multi-hop scenario.

In the first scenario, depth difference between the malicious node and the source node is $\Delta d \in [0, r]$ and azimuth angle is $\theta \in \left[\arcsin\left(\frac{\Delta d}{r}\right), \frac{\pi}{2}\right]$. The malicious node modifies Δd with $\Delta d + r$ during communication to interfere with the relay node's forwarding. Therefore, the relay node can identify the malicious node whose depth difference exceeds the hop radius. Assuming that the relay nodes are evenly distributed in the candidate area $S_c = \frac{\pi r^2}{2}$, the distribution approximate area S_{det} of the relay nodes that can identify position deception can be given as

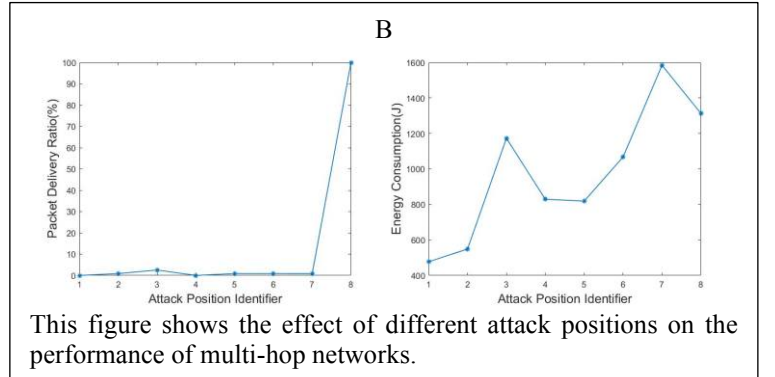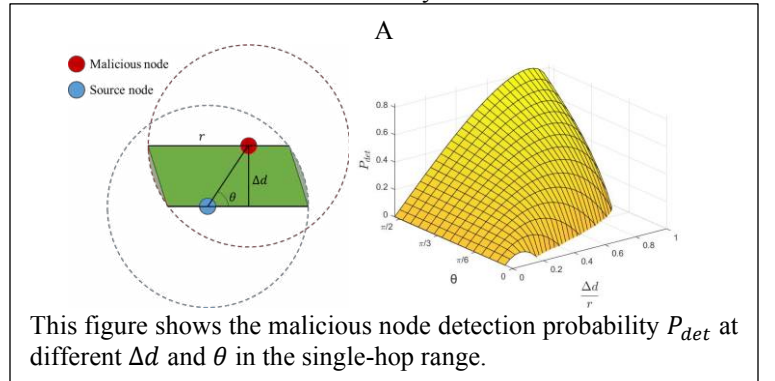$$S_{det} = \Delta d\sqrt{r^2 - \Delta d^2} - \Delta d^2 \cot\theta + r\Delta d. \quad (1)$$

Then the malicious node detection probability P_{det} in the single-hop range is

$$P_{det} = \frac{2}{\pi r^2}\left(\Delta d\sqrt{r^2 - \Delta d^2} - \Delta d^2 \cot\theta + r\Delta d\right). \quad (2)$$

As shown in figure A, P_{det} reaches its maximum value around $0.87r$, meanwhile, $\theta = \frac{\pi}{2}$.

In the multi-hop scenario, 30 nodes are randomly deployed in the network, where the depth difference between the source node and the sink node is 2 km and $r = 0.5$km. To evaluate the impact of location spoofing, eight attack positions with a depth difference of 0.2 km are evenly selected along the line from the source node and the sink node. As shown in figure B, except for position 8, where sink is reachable with a single hop, the packet delivery ratio (PDR) of malicious nodes is near to zero. Meanwhile, the overall network energy consumption increases with the gradual approach to sink.

In this extended abstract, we investigate location spoofing attacks of UASNs using OR. In a single-hop scenario, the network has the best security performance when $\Delta d \approx 0.87r$ and $\theta = \frac{\pi}{2}$. In the multi-hop scenario, the position slightly greater than r from the sink node is more vulnerable.

This figure shows the malicious node detection probability P_{det} at different Δd and θ in the single-hop range.

This figure shows the effect of different attack positions on the performance of multi-hop networks.

[1] Jiang, S. On securing underwater acoustic networks: A survey. IEEE Commun. Surv. Tutor. 2019, 21, 729–752.

[2] Mageswari, R. U.; Baulkani, S. Routing technique for data transmission under jammer in multi-hop wireless network. J. Ambient Intell. Humanized Comput. 2021, 12, 3705–3713.

[3] Yan H, Shi Z, Cui J, DBR, Depth-based Routing for Underwater Sensor Networks [J]. In: Proceedings of IFIP Networking '08.